Nanoscale Advances

Accepted Manuscript

View Article Online
DOI: 10.1039/D4NA00572D

A Review on recent progress in polymer composites for effective electromagnetic interference shielding properties- Structures, Process, Sustainability approaches

Rajesh Kumar Bheema[1], Krithika Bhaskaran[1], Akshat Verma[1], Gopu J[1], Murthy Chavali[2] and Krishna Chaitanya Etika[1]*

[1] Department of Chemical Engineering, BITS Pilani, Pilani, Rajasthan 333 031, India
[2] Office of the Dean Research, MIT World Peace University, Survey No, 124, Paud Rd, Kothrud, Pune, Maharashtra 411038, India

* Corresponding author emails: etika.krishna@pilani.bits-pilani.ac.in

Abstract

The rapid proliferation and extensive use of electronic devices have resulted in a meteoric increase in electromagnetic interference (EMI), which causes electronic devices to malfunction. The quest for the best shielding material to overcome EMI is boundless. This pursuit has taken different directions, right from materials to structures to process up to the concept of sustainable materials. The emergence of polymer composites has substituted the metal and metal alloy-based EMI shielding materials due to their unique features such as lightweight, excellent corrosion resistance, superior electrical, dielectric, thermal, mechanical, and magnetic properties that are beneficial for suppressing the EMI. Therefore, polymer nanocomposites are an extensively explored EMI shielding materials strategy. This review focuses on recent research developments with major emphasis on structural aspects and processing in enhancing the EMI shielding effectiveness of polymer nanocomposites with their underlying mechanisms and some glimpses on the sustainability approaches taken in this field is deeply reviewed.

Keywords: Polymer Composites, EMI Shielding, Sustainability

1 Introduction

View Article Online
DOI: 10.1039/D4NA00572D

Electronic communications technology has significantly improved over the years, and a variety of electrical devices are now widely employed in several sectors such as communications, civic, aircraft, military, and others.[1] Furthermore, these electronic devices emit electromagnetic (EM) waves continuously during operation, resulting in electromagnetic interference (EMI) between electrical appliances that have a detrimental impact on the operational accuracy of electronic equipment in the electronic industries.[2] However, EMI has become a new form of pollution due to the proliferation of electronic devices in the past few decades. The effects of this EMI can cause service interruption, data loss, permanent damage to equipment, and failure.[3] Owing to such issues, the expedition investigated several methods for preparing EMI shielding materials in the quest for the perfect shielding material.

Metals are excellent conductors of electricity and may reflect EM waves; hence, metals are widely used in EMI Shielding applications.[4], [5], [6], [7] However, the shielding mechanism in metals is dominated by the reflection of EM waves, which is not always a desirable option.[4], [5] In addition, relatively large densities and high production costs limit their extensive EMI shielding applicability.[8], [9] Due to these limitations of metals researchers focused on using polymers for EMI shielding applications because of their properties such as light weight, flexibility, low density, ease of processing, chemical and thermal stability, and most importantly, scalability. The polymers mostly allow the EMI waves to pass through the surface for absorption phenomena to happen rather than reflection, which occurs in metals. [10] Polymer nanocomposites (PNC) represent a class of materials that possess a unique combination of electrical, thermal, dielectric, magnetic, and/or mechanical properties.[4]–[7], [11] PNC characteristics may be tailored for EM wave suppression depending on the type of polymer and filler utilized. Due to their appealing properties, polymer nanocomposites have been considered an alternative to metals for EMI shielding applications.[4], [5], [12]

Furthermore, polymer-based composites containing lossy dielectric materials and/or magnetic materials are used to eliminate EMI and protect electronic devices from unwanted EM waves through absorption and reflection. In general, absorption dominant

View Article Online
DOI: 10.1039/D4NA00572D

shielding materials are preferable for equipment over reflection, because reflection can cause additional interference to nearby equipment [13]. To mitigate these problems caused by signal interference, efficient shielding materials are required to defend the normal operation of electronic systems. Furthermore, EMI shielding materials should have desirable characteristics such as low density, large absorption capability, thin, lightweight, and wide-range frequency bandwidth [14]. In addition, the selection of materials will also play important role in the designing of EMI shielding material. Recent studies have demonstrated the growing demand for low-cost and efficient EMI shielding materials as a consequence of the greater usage of electronic devices and electrical systems in industrial applications in the microwave frequency range. [15]–[18]. Furthermore, several studies on thin, lighter weight, effective shielding materials suitable for large bandwidth absorption have been reported[19]–[23]. Furthermore, effective polymeric EMI shielding materials containing carbon-based fillers and metals-based fillers, and conducting polymers have been reported in the literature [4]–[7], [11],[24], [25]. However, poor dispersion, phase separation, and high filler content are the main challenges in these studies. Owing to such limitations, various structural and processing strategies have been developed to achieve efficient EMI shielding materials [26]–[30]. This paper provides a comprehensive overview of structural and processing strategies for polymer-based composites for electromagnetic interference (EMI) shielding.

1.1 Scope of the review

Polymer-based EMI shielding materials have been developed using a variety of processing methods, as reported in the literature. Initially, EMI shielding materials are prepared by adding the essential filling materials such as conductive, magnetic, and dielectric materials, either alone or in combination, into the polymer matrix. Again, this strategy challenged to achieve the desired EMI shielding performance due to poor dispersion, phase separation within the matrix, and other drawbacks such as high filler content [26]–[30]. However, the excessive filler content results in the expected shielding but reduces the mechanical properties of the composites [12]. These challenges have resulted in refinement and renaissance of the research approach in polymer nanocomposites toward various structural strategies of nanomaterials and processing strategies of composites. This study

View Article Online
DOI: 10.1039/D4NA00572D

also includes glimpses of research exploring biodegradable, longer lasting, and self-healing materials that nurture sustainability in the EMI shield materials. This review mainly focuses on recent research developments, with a particular emphasis on structural aspects and processing in enhancing the EMI shielding effectiveness of polymer nanocomposites and their underlying mechanisms, as well as some glimpses into the sustainability approaches included in this field. The outcome of this study will help to understand the aspects and material properties such as electrical conductivity (σ), magnetic permeability (μ), dielectric permittivity (ε), and shield thickness (t) that influenced the EMI shielding performance as shown in Fig. 1.

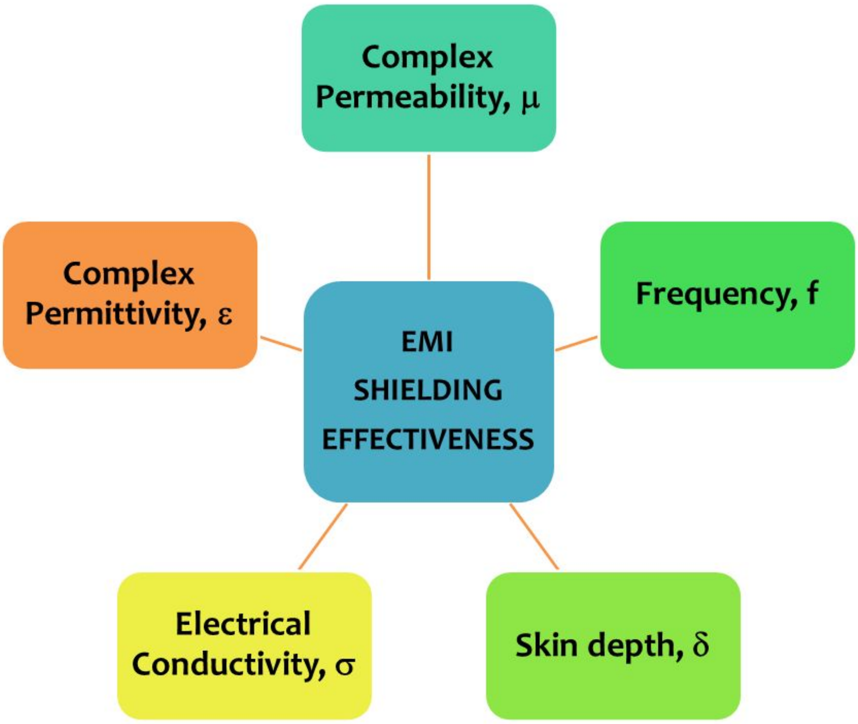

Fig. 1. Factors affecting the EMI shielding characteristics of the polymer composites.

2 The basic theory of EMI shielding mechanism:

The EMI shielding effectiveness is the primary metric for determining the performance of EMI shielding material, which evaluates the EM wave's attenuation by the shield. However, the attenuation of incident EM waves is primarily achieved by a combination of reflection, and/or absorption, which exists due to mobile charge carriers and electric and magnetic dipoles within the material [31]. When an EM wave is incident on the surface of shielding

View Article Online
DOI: 10.1039/D4NA00572D

material, an EM wave's energy from the shield will be partly reflected and partly absorbed. The residual energy is neither reflected nor absorbed by the shield but is the energy that emerges from the shield, as shown in Fig. 2.

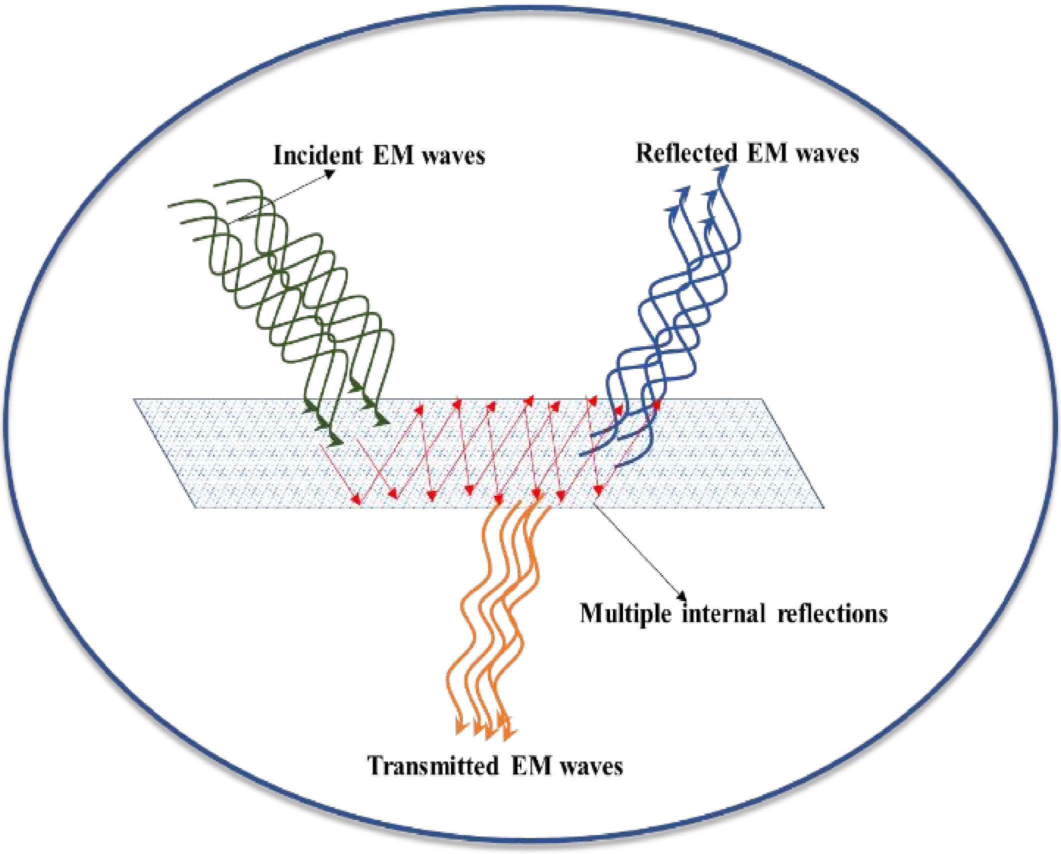

Fig.2: Pictorial depiction of the mechanism of an EMI shielding material

The attenuation of EM waves occurs mainly by three major mechanisms, namely reflection (R), absorption (A), and multiple internal reflections (MR). A two-port vector network analyzer (VNA) recorded the scattering parameters such as S_{11}, S_{12}, S_{21}, and S_{22} which can be correlated to the reflection, absorption, and transmission coefficients.

$$T=|\frac{P_T}{P_I}| = |\frac{E_T}{E_I}|^2 = |S_{12}|^2 = |S_{21}|^2 \quad (1)$$

$$R= |\frac{P_R}{P_I}| = |\frac{E_R}{E_I}|^2 = |S_{11}|^2 = |S_{22}|^2 \quad (2)$$

$$A= 1-R-T \quad (3)$$

View Article Online
DOI: 10.1039/D4NA00572D

Where P_T (E_T), P_R (E_R), and P_I (E_I) are the power densities of the transmitted, reflected, and incident of EM waves, respectively.

The total EMI shielding effectiveness (SE_T) of a particular material is defined as the efficiency of the barrier material in attenuating EM waves, and it includes losses due to EM waves reflection and absorption and is expressed in terms of SE_T [31] as follows:

$$SE_T\,(dB) = SE_R + SE_A + SE_M \tag{4}$$

$$SE_T\,(dB) = SE_R + SE_A = 10\log(1/T) = 10\log(1/S_{21}^2) \tag{5}$$

$$SE_R = 10\log(1/(1-R)) = 10\log(1/(1-S_{11}^2)) \tag{6}$$

$$SE_A = -10\log(T/(1-R)) = -10\log\,(S_{21}^2 / (1-S_{11}^2)) \tag{7}$$

where SE_A, SE_M, and SE_R are the shielding effectiveness (SE) due to absorption loss, multiple internal reflection loss and reflection loss. Generally, SE_M was negligible when SE_T was more than 10 dB [2], [3]. SE_M can be related to the microwave scattering effect caused by the distribution of conductive and magnetic particles, dielectric polarization, and interfacial polarization, which helps to reduce the intensity of electromagnetic waves entering the material due to the impedance mismatch between air and the material surface. [32]

3 Structure-based strategies of nanomaterials for the fabrication of efficient EMI shielding materials

The electromagnetic theory explains that an impedance match between the shielding material's surface and the incident EM wave results in greater wave penetration. To ensure effective wave interaction, the shield should have adequate electrical conductivity [4], [6], [7]. Subsequently, a conductive material and/or a hybrid of magnetic-dielectric materials were introduced [33]–[38]. The dual benefit of nanofiller produces additional effects such as high multiple-interface polarisation, all of which are useful in increasing shielding effectiveness[4], [7]. Previously, several researchers published numerous studies on structure-based strategies for the fabrication of EMI shielding materials, as seen in Table 1. The numerous strategies developed with different structures, such as hybrids (e.g., Fe_3O_4 decorated on Graphene nanoparticles or Multiwalled Nanotubes), core-shell (e.g., Fe_3O_4 @ MWNT), and layered structures, contain various types of nanofillers. A good EMI

View Article Online
DOI: 10.1039/D4NA00572D

shielding material should have good complex permeability and permittivity. In the composites, combining these used nanofillers has improved the dielectric loss and the magnetic loss. The increased EMI shielding effectiveness in composites containing structure-based nanoparticles can be attributed to the combined effects of dielectric losses coupled with the magnetic losses arising due to the presence of structure-based nanoparticles [39]–[41]. The structure-based strategies can significantly increase the complex permittivity and permeability of polymer composites, thereby increasing the shielding performance of EMI shielding materials [39]–[41]. Furthermore, the structural refinement of nanofillers includes aspects such as doping/ substitution in the entire matrix or one of the fillers, enhancing the current property, or introducing new aspects of additional benefit for the fabrication of EMI shielding material. Henceforth, this review explains the various types of structure-based composites and their mechanisms adopted to achieve maximum EMI shielding. The main interest in this review paper discusses the role of hybrid nanoparticle combinations, the different layered structure, gradient structures, doped structures, and structures such as foams, aerogels and core-shell structures. The fundamental principles of segregated and template structures are also discussed.

3.1 Hybrid structures

3.1.1 Conductive hybrid structures

The first approach was to create a hierarchical structure containing materials with similar or distinct impedance properties that can attenuate incident EM waves. These structures include combinations of two or more conductive materials in the polymer composite. These hybrid structures were synthesized by physical mixing, synthesis of one filler in the presence of another, or co-synthesis of two or more fillers, which leads to the growth of decorated structure of one or more fillers on the surface [42], [43]. The dual benefit of nanofiller produces additional effects such as high multiple-interface polarisation, all of which are useful in increasing shielding effectiveness. ~~A good EMI shielding material should have good complex permittivity~~. In the composites, combining these used nanofillers has improved the dielectric loss. The increased EMI shielding in composites containing structure-based nanoparticles can be attributed to the effects of dielectric

View Article Online
DOI: 10.1039/D4NA00572D

losses arising due to the presence of structure-based nanoparticles. Previously, several researchers published numerous studies on hybrid structures and used them to fabricate the EMI shielding materials, as seen in Table 1.

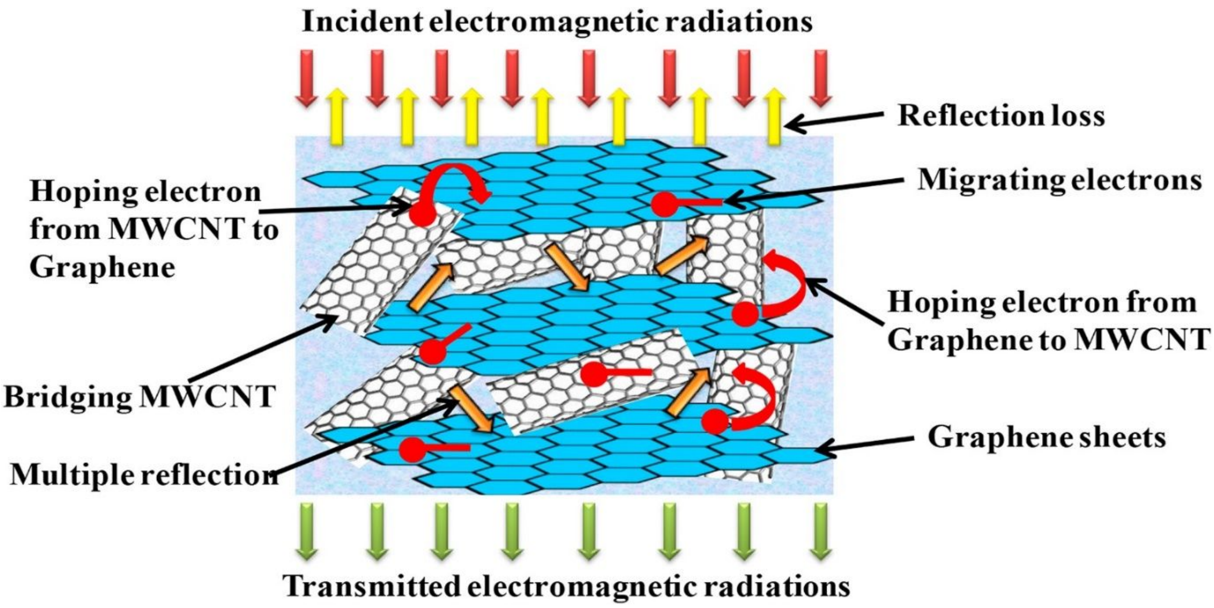

Fig.3: Schematic representation of the proposed EMI shielding mechanism in PUGCNT nanocomposites. Reprinted with permission. Copyright (2017) [44]

View Article Online
DOI: 10.1039/D4NA00572D

Table 1. EMI shielding values of conductive hybrid structures composites

Materials	Filler content	Conductivity (s/m)	SE_T (dB)	Frequency (GHz)	Ref
rGO-CF	0.75 wt%	7.13	37.8	8.2 -12.4	[43]
GNP-MWCNT	10 wt%	9.5	47	20-40	[44]
CNT/CF	0.35 wt%	0.8×10^{-3}	42	8.2 -12.4	[42]
MNPs@MWCNTs	4 wt%	1070	30-60	0.5-12.0	[45]
SSF-CNT	3.5vol%	100	47.5	8.2 -12.4	[46]
Polyamide-6/CNT	0.3 wt%	100	25	8.2 -12.4	[47]
PANI/CNT	25 wt%	1907	27.5-39.2	12.4-18	[48]
PCL-MWNCT	0.25vol%	4.8	60-80	0.04- 40	[49]
Copper nanowires-thermally annealed graphene/epoxy	7.2 wt%	120.8	47	8.2-12.4	[50]
PDMS/0.43 wt% of rGO/0.33 wt% of AgNW	-	1210	34.1	8.2-12.4	[51]

3.1.2 Magnetic and conductive materials hybrid structures

The second approach is to employ a hybrid structure with a combination of magnetic or dielectric material and a conductive filler in the polymer composite for the enhancement of EMI shielding efficiency. Subsequently, the addition of conductive material along with magnetic or dielectric materials generates the dual benefit of nanofiller and produces additional effects such as high multiple-interface polarisation, all of which are useful in increasing shielding effectiveness. In addition, it is well known that two parameters, i.e., magnetic loss and dielectric loss, primarily influence EM wave absorption. In the EMI shielding materials, combining magnetic material with conductive nanofillers has improved the dielectric loss and magnetic loss. In order to create induced magnetic and dielectric losses, a suitable EMI shielding material should have high complex permeability and permittivity. Complex permittivity and permeability are caused by dipole polarization, electronic polarization, natural resonance, magnetic dipoles, magnetic losses, eddy, and hysteresis losses, in which crystal structure, size, and morphology may play a vital role. The increased EMI shielding in composites containing structure-based nanoparticles can be attributed to the combined effects of dielectric losses coupled with the magnetic losses arising from structure-based nanoparticles [4], [7]. Therefore, many researchers have focused specifically on the complex hybrid structure of nanofillers to fabricate an efficient EMI shielding material, which is listed in Table 2.

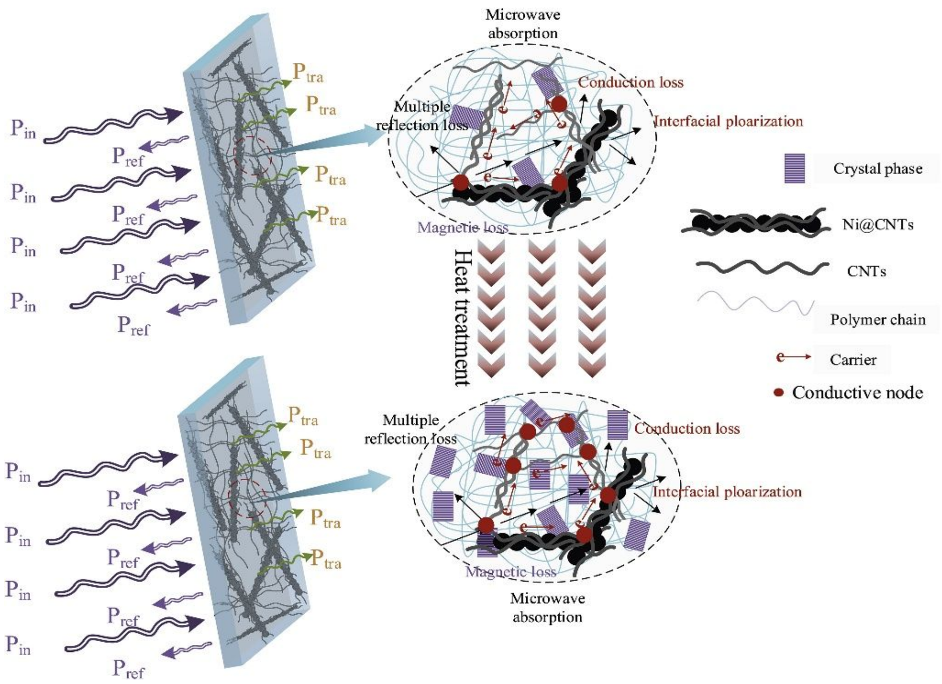

Fig.4: A schematic illustration of the distribution of the conductive filler in PVDF/CNTs/Ni@CNTs flexible composite films before and after heat treatment. Reprinted with permission. Copyright (2019) [52]

Table 2. EMI shielding values of conductive and magnetic hybrid structures composites

Materials	**Synthesis Method**	**Conductivity (S/cm)**	**Thickness (mm)**	**Polymer matrix**	**SE_T (dB)**	**Frequency (GHz)**	**Ref**
PANI/15 wt% $BaFe_{12}O_{19}$ (BF)	Co-precipitation	0.34	2	PANI	19.7	2-18	[53]
PANI/28 wt% $Mn_{0.5}Zn_{0.5}Fe_2O_4$			2	PANI	6-20	0.03-1	[54]
3% Graphene decorated with Nickel NPs	Co-precipitation	3.10×10^{-4}	1	Polybenzoxazine	>20	8.2 -12.4	[55]
10 wt% CNT/12 wt% Ni@CNT	Magnetic field-supported solvothermal process	2.57	0.5	PVDF	51.4	12.4-18	[52]
O-FeCo- diamine monomer 4,4′-diamino diphenyl methane, MWCNT	*Insitu* reduction using a solvothermal process	1×10^{-3}		PVDF	41	12.4-18	[56]
10 wt% Fe_3C-carbon	Carbonization of melamine and iron salt			PVDF	35	14-18	[57]
90:10 ratio of Fe_3O_4 and carbon black (CB)		10		Natural rubber	14.7 -23.1	1-12	[58]
0.25vol% of Fe_3O_4-MWCNT			5	Polycarbonate (PC)/PVDF	38	18	[59]
0.25vol% of Fe_3O_4-MWCNT			5	PC/PVDF	30-36	8-18	[60]
0.15 vol% $NiFe_2O_4$-MWCNT			5	PC/PVDF	19.7	2-18	[60]
0.28 vol% $CoFe_2O_4$-MWCNT			5	PC/PVDF	6-20	0.03-1	[60]

Modified Gr nanoplatelets and MWCNT-Fe_3O_4			Polyurethane	27.5	8 -12.4	[61]
Fe_3O_4-CNT	9×10^{-3}	1.1	PVDF	32.7	18-26	[62]
Fe_3O_4-GNP	2×10^{-2}	1.1	PVDF	35.6	18-26	[62]
rGO@Fe_3O_4- MWCNT	1.8×10^{-3}	5	PC/polystyrene	> 30	8-18	[63]
0.5 wt% rGO deposited with carbon fiber-Fe_3O_4 -9 wt% modified rGO	11.04	7	Epoxy matrix	> 30	8.2-26.5	[64]
rGO-Fe_3O_4	7×10^{-4}		PC matrix	28	8-18	[65]
rGO-Fe_3O_4	4×10^{-4}		PC matrix	33	8-18	[65]
wt% CNT-5 wt% rGO-Fe_3O_4			PC matrix	43.5	8 -12.4	[66]
45 wt% $NiFe_2O_4$-5 wt% rGO	2.16×10^{-12}	2	Propylene	28.5	5.8-8.2	[67]
$NiCoFe_2O_4$ (NCF)- CB	1.513×10^{-4}	1.5	Polyvinyl Alcohol (PVA)	27	8-18	[68]

View Article Online
DOI: 10.1039/D4NA00572D

3.1.3 Magnetic-Dielectric-Conductive hybrid structures

The third approach is to create a hierarchical structure in the polymer composite containing a combination of magnetic and dielectric materials along with a conductive filler. In these hierarchical structures, decorating magnetic nanoparticles on dielectric materials or vice versa facilitated a protective encapsulation of decorated nanoparticles on the surface of other nanoparticles to prevent agglomeration of the nanoparticles [69]. Previously, the researchers reported that magnetic nanoparticles decorated on dielectric nanoparticles have better dielectric properties than dielectric nanoparticles decorated on magnetic nanoparticles because of increased O-vacancy concentration (Oxygen vacancy concentration refers to a defect caused by a decrease in oxygen content, leading to an increased number of oxygen vacancies. These vacancies significantly influence the structural, physical, and electrical properties of the material) in dielectric nanoparticles of larger grains and O-vacancy-induced enhancement in interfacial polarisation between the dielectric nanoparticles and magnetic nanoparticles, respectively [70]–[73].

Recent studies have investigated that dielectric materials, including, SnO_2, TiO_2, ZrO_2, ZnO, Al_2O_3, carbon materials, and polymers, are used as a dielectric source to impart dielectric losses and are used alone or in combination with magnetic and conductive materials [74]. For example, Biswas et al. synthesized graphene oxide sheets decorated with $BaTiO_3$ and Fe_3O_4 nanoparticles. These nanoparticles are combined with modified MWNT and embedded in the Polycarbonate (PC)/Polyvinylidene fluoride (PVDF) matrix. The nanocomposite reported SE_T values of 32.5-35 dB over the frequency range of 12-18 GHz. It can be observed that the composites demonstrated an increase in SE_T values due to the synergistic effect of hybrid lossy materials and selective localization of Graphene oxide (GO) in PC and MWNT in PVDF, which retains the electrical conductivity of composites [74]. The authors also fabricated composites through multilayer assembly, in which outer layers with modified $BaTiO_3$/Fe_3O_4 co-doped GO/modified MWCNT/PC/PVDF composite and inner layers with modified MWCNT/PVDF in the composite [74]. The authors also reported that the SE_T values of composites fabricated through multilayer assembly further increased to 46 dB over the frequency range of 12-18 GHz.

View Article Online
DOI: 10.1039/D4NA00572D

Jin et al. synthesized a hybrid structure made of graphene nanoplate along with Fe_3O_4 decorated on $BaTiO_3$ (GFBT) in two steps hydrothermal process. The $BaTiO_3$ particles of 20 nm are primarily coated on the Fe_3O_4 nanospheres forming the hybrid structure of Fe_3O_4 and $BaTiO_3$. The hybrid structure contained $BaTiO_3/Fe_3O_4$ nanoparticles of about 200 nm diameter anchored on the surface of graphene were used along with MWNT in methyl vinyl silicone rubber. The composite containing 16 wt% with the ratio of 1:5 of MWNT: GFBT filler loading exhibited SE_T values of 26.7 dB in the frequency range of 1-20 GHz for a sample thickness of 2.6 mm [75]. Sambyal et al. reported an encapsulated polypyrrole composite with the combination of rGO, Fe_3O_4 and barium strontium titanate (BST) nanoparticles. The BST/rGO/Fe_3O_4 (BRF) hybrid was synthesized by co-precipitation. In this process, the precursors rGO and BST nanoparticles were added to the precursor solution of Fe_3O_4, thus forming the hybrid structure of nanoparticles. The hybrid composite showed an EMI SE of around 48 dB for a thickness of 2.5 mm in the X-Band frequency range [76].

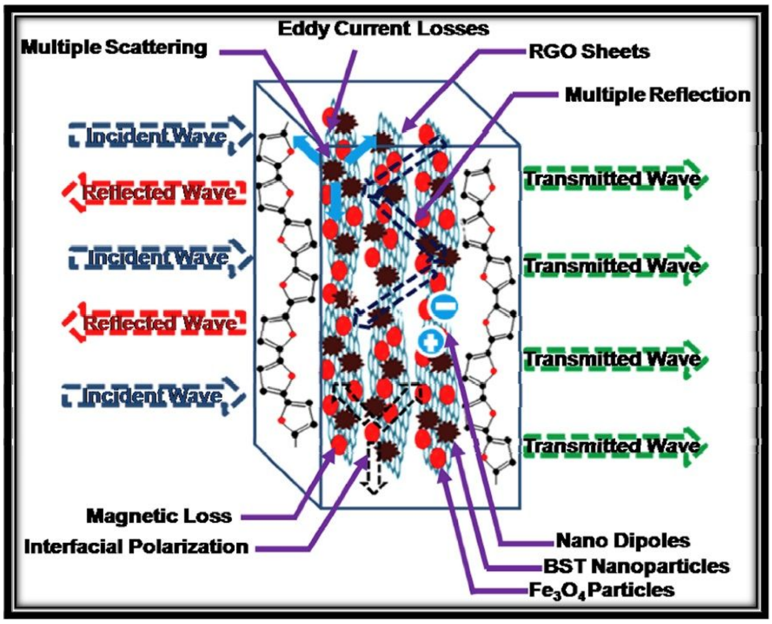

Fig.5: Schematic representation of possible mechanism of EMI Shielding in PBRF composite. Reprinted with permission. Copyright (2018) [76]

3.2 Layered Structures

The layered structures provide ultralight, low density, flexible, scalable, and highly conductive micrometer-thick EMI shields that can be made using standard polymer processing methods for flexible, wearable, and smart electronics. The production of

View Article Online
DOI: 10.1039/D4NA00572D

multifunctional EMI shields is the major challenge to be addressed. The industries require EMI shields that not only limit the detrimental impacts of EM waves but also have exceptional mechanical and thermal properties [77], [78]. The second major challenge is the necessity to manufacture EMI shields that absorb a large amount of the incoming EM waves. Furthermore, several research studies have only focused on the development of highly conductive EMI shields that rely heavily on EM wave reflections. However, this strategy is undesirable for military and medical applications that demand a high level of EM wave absorption with minimum reflections. Indeed, EM waves reflected from a conductive EMI shield can serve as a secondary source of EMI, affecting the operation of neighbouring electronics.

The manufacturing of multilayer EMI shields has recently been suggested as a potential strategy to decrease reflection and increase EM wave absorption. A multilayer structure comprising suitable nanomaterials and polymers was used to create multifunctional EMI shields with excellent EMI shielding properties. Furthermore, it has been demonstrated in several investigations that a layered structure of conductive and magnetic materials may significantly improve the absorption component of the shielding and, to a large degree, the overall EMI shielding effectiveness (EMI SE) of developed structures. This study concisely described the main ideas of EMI shielding, as well as the underlying shielding mechanisms of multilayer shields, and then provided a complete evaluation of fascinating multilayer shield research.

The current state-of-the-art is to prepare a multilayer structure EMI shielding material with softness, durability, rapid thermal dissipation, and desirable resilience and endows the composites with excellent shielding effectiveness [79]. Layered structures, such as sandwich structures, have been proven to be an effective strategy for attenuating EM waves. Furthermore, the layer-by-layer (LbL) assembly is a reliable process for making thin-film materials, which is used to build the layered structure composites required for EMI shielding applications. Therefore, this process was utilized to manufacture multilayer structured coatings for high-efficiency EMI shielding [79]. The multilayer structure, comprised of various conductive with different impedances or conductive and/or magnetic materials, creates unique interfaces among the materials that generate multiple internal reflections for EM waves, thereby boosting EMI shielding performance.

View Article Online
DOI: 10.1039/D4NA00572D

In addition, a few efforts have been made to produce highly efficient multilayer composites for EMI shielding applications. These studies reported that multiple internal reflections prevailing shielding mechanisms, impedance mismatch, and dielectric losses improved the shielding effectiveness. The preparation methods for producing thin-film composites in the form of multilayer stacks have been developed, and considerable work has already been published and is listed in Table 3. Layered structure composites are categorized based on a physical assembly of layers, self-assembled layered or in-situ layered structures with different combinations of fillers and different matrices.

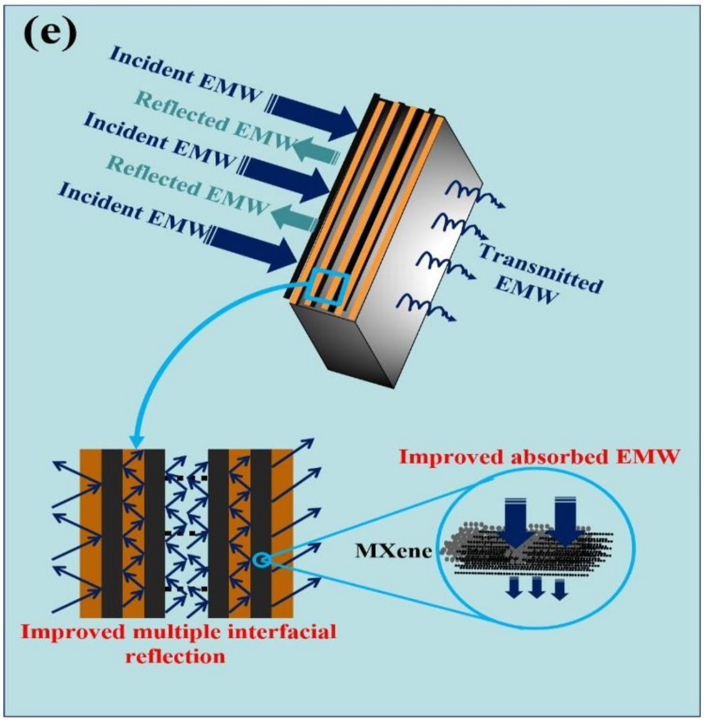

Fig.6: Schematic of electromagnetic microwave dissipation in the PVA/MXene multilayered films. Reprinted with permission. Copyright (2020) [78]

DOI: 10.1039/D4NA00572D

Table 3 The layered structure composites and their EMI shielding effectiveness values

Materials	Thickness (mm)	Conductivity (S/m)	SE_T (dB)	Frequency (GHz)	Ref
PP-MWCNT/PP-MA/10wt% PVA-2wt%MWCNT	1	0.03	36.7	1-2	[80]
PP-MWCNT/PP-MA/10wt%PVA-2wt% Gr Sheets	1	21	24.5	1-2	[80]
Cellulose/PET Oxide-CNT	0.15	20	35	8-12	[81]
PPEK/MWNT	11	39	61.5	8-12	[82]
MWNT/PMMA	0.3	1.5	40	8.2-12.4	[83]
SWNT/Cellulose	0.03	-	40	12-18	[30]
PVDF/GNP-Ni-CNT	0.6	0.15	46.4	12.4-18	[85]
T-ZnO/Ag/WPU	0.25	63500	87	8.2-12.4	[86]
GO/ PHDDT	0.02-4	-	37.92	8-12	[87]
CNT/BN/Rubber	1.4	98	31.38	8-12	[88]
PVDF-MWCNT-Mn-Fe3O4/Ni-C-PVDF	0.6	-	58	12-18	[89]
PC/PVDF with MWCNT-Fe_3O_4	0.9	1.1×10^{-4}	64	12-18	[90]
PVDF/CoNi/MWNT	0.95	1	41	20-40	[91]
Ni@nylon mesh/PP	2.5	2.26	50.6	8-12	[92]
PC/Ethyl Methyl acrylate/MWCNT/GNP	-	1.91×10^{-1}	34	8.2-12.4	[37]
PANICNPS	10	7.6×10^{-1}	10-20	8	[93]

View Article Online
DOI: 10.1039/D4NA00572D

Fe_3O_4@rGO/T-ZnO/Ag/WPU	0.5	22700	87.2	8-12.4	[94]
FeCo@rGO/Ag/WPU	0.3	1428.57	50.5	2-18	[95]
FeCo@ rGO/Ag/NWF/WPU	0.1	60000	77.1	2-18	[96]
Silicon Rubber /Ag@HGMs/ Fe_3O_4@CNT	2	279.3	59.39	8-12.4	[97]
FeCo@rGO/EbAg/WPU	-	-	84.8	8-12.4	[98]

3.3 Gradient / graded structures

EMI shielding materials that are lightweight, flexible, and readily functionalized offer greater application possibilities in a wide range of applications such as portable electronics and wearable materials. To achieve this, gradient layered structures have been created by layering polymer nanocomposites and increasing or decreasing the concentration of fillers layer by layer from the EM wave incident layer [6]. This gradient structure strategy can facilitate to create an extremely efficient EMI shielding material with low reflection. However, this gradient structure is mostly constrained by the manufacture of films and solid composites; few studies have been undertaken on creating gradient structures for composites using simple protocols.

Xu et al. have prepared flexible waterborne polyurethane (WPU) composite films by developing gradient structures as the density difference among rGO@Fe_3O_4 and T-ZnO/Ag nanoparticles [6]. These gradient structures demonstrated significant EMI shielding performance of 87 dB with as low as 39 % reflection power. The reflection power value of the Fe_3O_4@rGO/MWCNT/WPU composites may be reduced to 27% [6]. This suggested that the gradient structure containing both electric and magnetic materials reduced their reflection power in the gradient structure by regulating rGO content. H.J. Im et al. designed a multilayer graded structure by incorporating fillers of GNP and Ni in the Polymethyl methacrylate (PMMA) matrix. Firstly, the Ni was reduced onto GNP and then incorporated into PMMA [99]. The gradient structure consisted of 0.83 mm thick three layers, where the top layer containing the concentration of GNP/Ni filler loading increased by 20 wt%. The intermediate layer contains 30 wt% filler loading, and the bottom layer

View Article Online
DOI: 10.1039/D4NA00572D

contains 40 wt% filler loading. The gradient structure exhibited an EMI SE value of 61 dB over the X-band frequency range of 8-12.4 GHz. The gradient structure has demonstrated 3 orders higher than a monolayer of 2.5 mm thick containing 30 wt% GNP/Ni filler loading. The authors attributed the abrupt increase in filler loading by 10 wt% have helped to develop conductivity network structure between layers in the direction of propagation of EM wave. It can create additional multiple internal reflections between the stacked layers. It can also observe that the top layer containing lower filler loading supports better impedance matching and reduce surface reflections. It can enhance the absorption of EMI waves in the gradient structure [99]. A Sheng et al. designed a conductive gradient structure for reducing reflections in the hybrid system [100]. The gradient structure was constructed by three layers of Fe_3O_4@rGO. The rGo filler loading was increased from the top layer to the bottom layer in the gradient structure and the final layer containing MWNT in the WPU matrix. The gradient structure exhibited an EMI SE value of 35.9 dB for composite containing 11.2 wt% Fe_3O_4@rGO-30 wt% MWNT-WPU composite over the X-band frequency range of 8-12.4 GHz [100]. The composites containing gradient structures have enhanced the EMI SE value and were listed in Table 4.

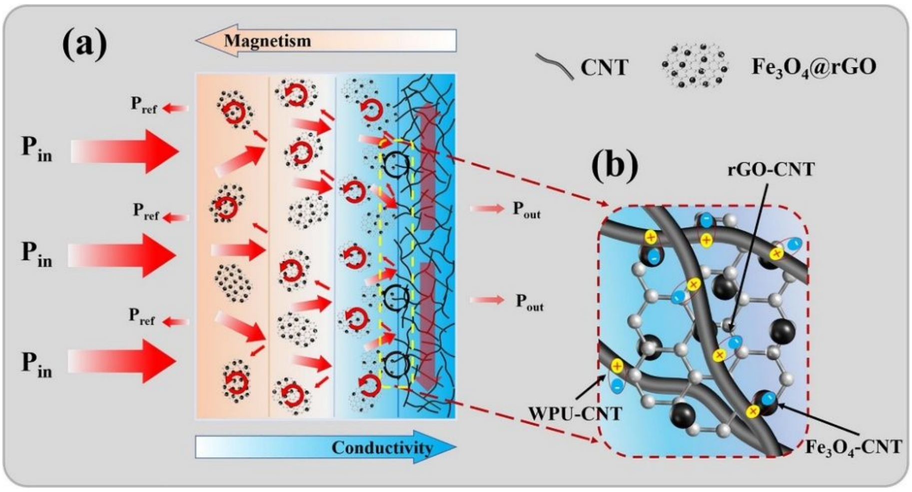

Fig.7: EMI shielding mechanism of the Fe3O4@rGO/MWCNT/WPU composite. Reprinted with permission. Copyright (2020) [100]

View Article Online
DOI: 10.1039/D4NA00572D

Table 4. Gradient structures composites and their EMI shielding effectiveness

Materials	Thickness (mm)	Conductivity (S/m)	SE_T (dB)	Frequency (GHz)	Ref
GNP/Ni/PMMA	2.5	-	61	8-12	[99]
WPU/Fe_3O_4@rGO/MWCNT	0.8	3.75	35.9	8-12	[100]
3 layers of SWCNT/ Vinylidene Fluoride	1.12	-	-6	35	[101]
Ti_3SiC_2-γ-Al_2O_3 /SiC	46	1000	50	8.2-12.4	[102]
CNT/SiO_2	5	-	-30	8-12	[103]
Fe/Al-Fe/Fe	1	0.16	70-80	0.03 – 1.5	[104]

3.4 Doped structures

The doping of EMI shielding materials and their enhancement strategies can be divided into three categories: i) doping excellent conductive nanofillers, ii) increasing the loading content of nanofillers and iii) approaching the homo dispersity of nanofillers in polymer-matrix. Despite substantial research on the fabrication of EMI shielding materials, the true potential of doped structures for this use has yet to be investigated. The doping of nanofillers such as graphene helps to retain the sp^2 electronic structure by increasing the electrical conductivity of doped structures [105]. Currently, n-type doping of carbon-based nanofillers such as graphene with heteroatoms such as nitrogen was proposed as a viable method for recovering graphene's electronic properties. Furthermore, sulfur is a comparatively recent n-type dopant, and its ability for applications apart from electrochemistry has yet to be thoroughly investigated. Zhou et al. and Denis et al. studied that S-doped graphene produces a thiophene-like structure that has a favorable effect on graphene's magnetic and electronic properties [106]. This review reported that doped nanofillers in a laminated structure exhibit considerably larger EMI shielding effectiveness than the undoped laminate at minimal thicknesses. This observation is attributed to the n-doping effect of nanofillers, which improves the electrical conductivity of doped structures. The composites containing doped nanostructures have enhanced the EMI SE value and were listed in Table 5.

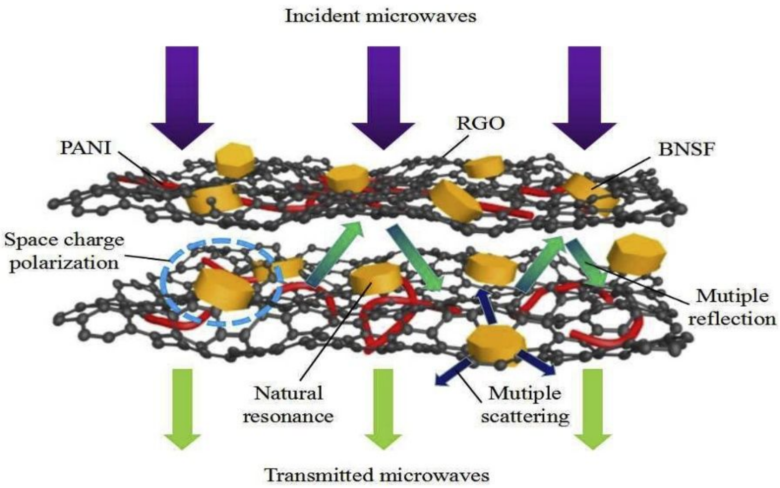

Fig.8: Schematic representation of the microwave attenuation mechanism in RGO/PANI/BNSF nanocomposites. Reprinted with permission. Copyright (2019) [107]

Table 5. Doped structures composites and their EMI shielding effectiveness

Materials	**Thickness (mm)**	**Conductivity (S/m)**	**SE_T (dB)**	**Frequency (GHz)**	**Ref**
$Ti_3C_2T_x$/c-PANI	0.04	2440	36	8-12	[108]
RGO/PANI/BNSF	2.90	-	50.5	2-18	[109]
p-TSA/PANI/GNPs	1.5	57.5	14.5	8-12.4	[110]
PANI/CSA-coated CNF	0.088	38.5	30	0-15	[111]
MWCNTs/sub-SF/ PANI	5	-	36	8-18	[112]
PC/sub-G/MWCNT	5	6.1×10^{-2}	33	8-18	[65]
N_2-doped graphene nanosheet - epoxy	2.4	-	40	8-12.4	[113]

View Article Online
DOI: 10.1039/D4NA00572D

Fe_3O_4/CCTO/P-gC_3N	1	-	30	8-12.4	[114]
PANI/Ni-Cd-Ferrite	2.3	4470	42.7	8-12.4	[115]
Silicone rubber /POE/ IL-MWCNT	1.2	0.14	25	8-12.4	[116]
TPU/sub-G	1	10	25	8-12.4	[117]
SBR/IL-MWCNT	5	10	35	2-18	[118]
PS/IL-MWCNT	1	0.01	7	8-12.4	[119]
Pyrrole/Nd-Co	2	-	15	8-12.4	[120]

3.5 Aerogel composites

Aerogels have emerged as one of the most interesting materials of the late 20th century. The innovative processing technique yields aerogel with remarkably high porosity, large specific surface area, low density, high dielectric strength, and low thermal conductivity, made these materials utilised in various applications such as aerospace, biomedical devices, energy storage, EMI shielding materials, sensors, and coatings [121]. Since Kistler invented the aerogel with silica, aerogels have been created from a wide range of materials, that includes metal oxides, biopolymers, resins, etc [122]. Furthermore, the addition of a range of nanomaterials into the aerogel matrix to construct composite with aerogels. Moreover, an aerogel network has pore diameters in the order of nanometers. The further addition of nanomaterials into an aerogel developed a composite with superior functional properties including increased specific surface area, improved mechanical strength, and better thermal and electrical conductivity. [123]

Since this first use of carbon nanomaterials in the production of an aerogel structure, the utilization of a variety of nanomaterials for the development of high-performance aerogel structures has grown exponentially. For example, carbon nanomaterials such as carbon nanotubes, graphene, and carbon nanofibers have been incorporated into aerogels to

View Article Online
DOI: 10.1039/D4NA00572D

improve the electrical conductivity and performance for applications such as supercapacitors, sensors, and batteries [124], [125].

In other earlier works, the lightweight 3D structure design is a primary prerequisite in EMI shielding applications. The actual EMI SE for lightweight porous materials was determined in terms of specific shielding effectiveness (SSE) and absolute shielding effectiveness (ASE), which define the accurate shielding performance of material by considering three factors: EMI SE, density (ρ), and thickness (t), which are calculated as follows,

$$SSE = SE_T/\rho \text{ dB cm}^3\text{g}^{-1}$$

$$ASE = SSE/t = SE_T/\rho t \text{ dB cm}^2\text{g}^{-1}$$

The pores developed in the lightweight 3D structure decrease the density of the material and are also supposed to increase multiple internal reflections of EM waves, increasing EMI SE values. Porosity has been integrated into the material to reduce the density of the EMI shielding materials to get the best of both SE and lightweight, and the impact of porosity on the properties and structure of porous materials has been adequately studied. Hu et al. investigated multifunctional aerogel films made with Kevlar fiber, carbon nanotubes (CNT) as reinforcing fillers, and hydrophobic fluorocarbon resin as polymer matrix. The final material comprises self-cleaning property due to the hydrophobic surface nature of the film, having good electrical conductivity leads to joule heating property and good EMI shielding property of 54.4 dB at a thickness of 546μm in the X-band region. (8-12GHz). [126]

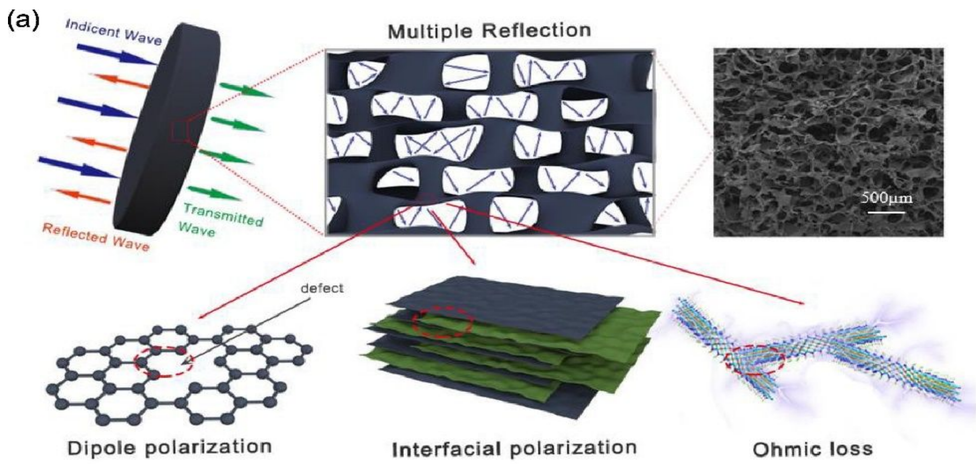

Fig.9: Possible electromagnetic shielding mechanism of $Ti_3C_2T_x$/RGO/ANFs hybrid aerogel. Reprinted with permission. Copyright (2022) [127]

Table 6. Aero gel composites and their EMI shielding effectiveness

Materials	Type	Method	Conductivity (S/m)	SE_T (dB)	Frequency (GHz)	Ref
PDMS/0.21 wt% rGO/0.07 wt% of SWCNT	Aerogel foams	Freeze drying method	120	31	8.2-12.4	[128]
0.51 wt% CNT/cellulose	Template	Ice-template freeze drying method	38.9	51	8.2-12.4	[129]
0.74 vol% $Ti_3C_2T_x$/Graphene/Epoxy	Nanocomposite	Hydrothermal assembly and freeze-drying	695.9	50	8.2-12.4	[130]
1.95 wt% PDMS/reduced graphene	Flexible foams	Freeze drying	65.6	43.6	8.2-12.4	[131]
Polyurethane(WPU)/Silver nanowire (Ag-NW)	Flexible nanocomposites	Freeze drying	587	64	8.2-12.4	[132]
0.8% graphene/epoxy	nanocomposite	Freeze drying and thermal annealing	980	32	8.2-12.4	[133]
0.2 wt%TAGAs/epoxy	nanocomposite	Freeze drying and thermal annealing	96	25	8.2-12.4	[133]
6.1 wt% MXene (Ti3C2Tx)/ sodium alginate (SA)	Aerogel	Freeze drying	2211	48.2	8.2-12.4	[134]
Nacre-mimetic graphene	Aerogel	Bidirectional freezing and freeze	0.5	65	8-12	[135]

(aerogel)/ PDMS		drying				
1.64 wt% $Ti_3C_2T_X$ MXene / epoxy	Foam	Sol-gel followed by freeze drying	184	46	8-12.4	[136]
0.33 wt% Graphene/ phenolic resin/epoxy resin	Aerogels	Hydrothermal	73	35	8-12.4	[137]

View Article Online
DOI: 10.1039/D4NA00572D

3.6 Foams

The polymer foams have gained great attention in the designing of EMI shielding materials due to the advantage of being lightweight, while the unique porous structure can effectively absorb EM waves by extending the travel path [25]. Foam composites demonstrated absorption-dominated shielding phenomena, which meets the present standards of EMI shielding applications. Furthermore, conductive polymer foams, carbon foams, inorganic metal foams and MXene foams are gaining popularity for use in EMI shielding applications. The primary goal of this review is to study the current state of research in the design of polymer composite foams as EMI shielding materials.

Zhang et al. used subcritical CO_2 ($scCO_2$) as a physical foaming agent to fabricate graphene-reinforced PMMA composite. The established multi-interface microporous structures have the potential to improve shielding effectiveness by allowing for multiple internal reflections and resolving the composites' pervasive brittleness [138]. Furthermore, Zhang et al. fabricated three-dimensional (3D) compressible foam with conductive Mxene sheets. The prepared conductive network was covered with a thin layer of elastic polydimethylsiloxane (PDMS) to increase mechanical robustness [134]. After 500 compression-release cycles, the PDMS-coated foam achieved a superior EMI SE value of 48.2 dB, demonstrating its remarkable ability for compressible and robust EMI shielding gaskets. Gupta et al. formulated a 2,20-azo isobutyro nitrile (AIBN), a chemical blowing agent used to prepare the CNT-PS foam composite. When heated, AIBN decomposed and released nitrogen gas inside the composite structure, providing adequate EMI shielding efficiency [139]. Shen et al. used a modified water vapour-induced phase separation method to create porous PVDF/MWNT/graphene composites [140]. Furthermore, syntactic foam is a foam composite of hollow fragments distributed in a matrix. Two techniques have been used, including the use of conductive hollow particles as fillers for syntactic foams and the addition of excess conductive filler to syntactic foams. Furthermore, the template process has been illuminated to manufacture foam-based shielding materials due to its ease of operation, controllable structure, and diverse alteration. The polymeric composition can be coated on the pre-construct conductive foam in reverse on the composite foam for EMI shielding. Foam-based structures were

View Article Online
DOI: 10.1039/D4NA00572D

boosting multiple reflections and so on. Similarly, processing aspects like modifications in blending techniques, layered assembling, and even irradiation process boost EMI shielding through uniform dispersions, sequential attenuation, etc. Herein, we attempt to bring in a consolidated review of recent research with insights on the structural and processing-based approaches and their combinations and their underlying mechanism that has boosted the EMI shielding performance. Several researchers prepared various foams and determined their EMI shielding effectiveness were listed in the Table 7.

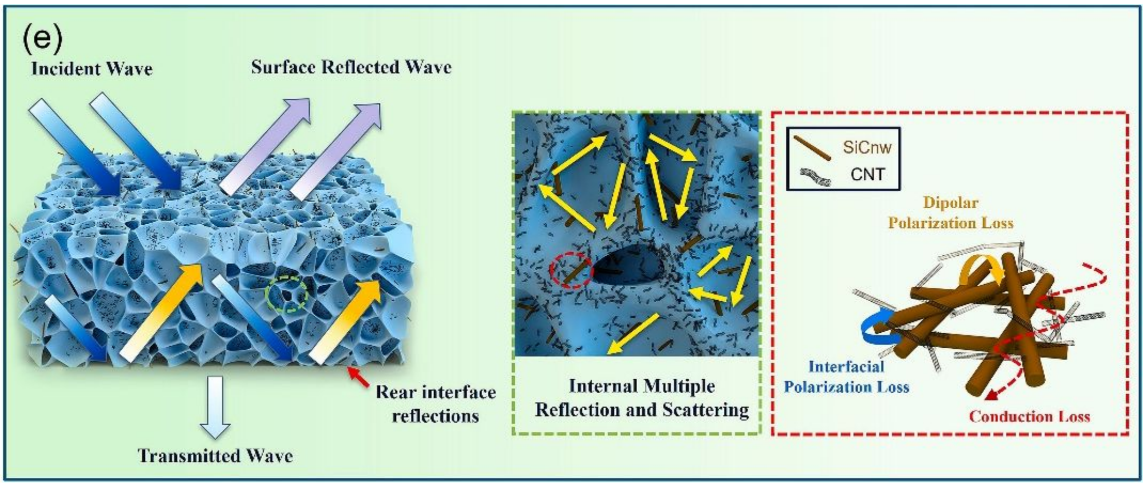

Fig.10: Schematic illustration of EM wave dissipation in the PVDF/CNT/SiCnw composite foams. Reprinted with permission. Copyright (2023) [141]

Table 7. Foam composites and their EMI shielding effectiveness

Materials	Thickness (mm)	Conductivity (S/m)	SE_T (dB)	Frequency (GHz)	Ref
TG-CN/PMMA	2	1	34	8.2-12.4	[142]
RG-CN/PMMA	2	0.1	19.5	8.2-12.4	[142]
GN-CN/PMMA	2	0.8	26	8.2-12.4	[142]
PVDF/Ni-chains	2	0.01	26.8	8.2-12.4	[143]
Silicone rubber/MWCNTs/Fe_3O_4	2	14.6	27.5	8.2-12.4	[144]
GO/NF/Epoxy	0.5	150	65	1-3	[145]
fMWCNTs/CTBN/Epoxy	2	0.43	22.90	12-18	[146]
PMMA/GNPs-MWCNTs	2	0.1	36	8-12	[147]
CNTs/PMMA laminated	2	-	36	8-12.4	[148]
GNPs/PMMA	2			8-12.4	[149]
EP/ZrP-MWCNT	2.2-2.5	3.02×10^{-4}	20.5	12-18	[150]
PMMA/Fe3O4@MWCNTs	2.5	2×10^{-4}	16	8.2-12.4	[151]
PMMA/MWCNT	3	-	-	8.2-12.4GHz	[152]
Microcellular Epoxy/MWCNT	2.8	1×10^{-7}	9	12-18GHz	[153]
PC/GNP	5	1×10^{-7}	39	8-12GHz	[154]

PVDF/MWCNT	1.7	0.44	34.1	18–26.5 GHz	[155]
PVDF/10 wt%GNP	3	0.52	37.4	26.5-40GHz	[156]
Silicone/30 wt%o-MWCNTs	6.4	-	73	12.4-18GHz	[157]
PU/31.3 wt%rGO	2.5	-	-50.8	2-18GHz	[158]
Epoxy/0.94vol%AgPs/0.44vol%rGF	3	45.3	58	8.2-12.4GHz	[159]
PDMS/2.7 wt%GF/2.0 wt%CNTS	2±0.05	31.5	833	8.2-12.4GHz	[160]

View Article Online
DOI: 10.1039/D4NA00572D

3.7 Core-shell structures

Core-shell nanoparticles are a special class of nanostructured materials that have gained a great deal of interest in the last two decades due to their unique characteristics and wide range of applications. A variety of "core-shell" nanostructures with tailorable characteristics may be generated by properly regulating the "core" and "shell", which can be utilised to build materials for EMI shielding. The primary goal of this study is to emphasise the fundamental notion of EMI shielding materials that have been discussed in the literature for various systems, as well as various synthetic and manufacturing methodologies for creating acceptable EM attenuation.

In this approach, the preparation of core@shell may be made of two distinct types of substance, such as inorganic@organic and vice versa, or of the same type of substance with different structures, such as inorganic@inorganic or organic@organic. The construction materials or the core or shell thickness ratio can modify the properties of these materials. The main drawback in the preparation of core@shell particles is a complex and time-consuming strategy.

Previously, a few researchers claimed that reinforcing core@shell particles in the polymer matrix can improve the polymer's complex permittivity and permeability. It can also help with impedance matching, which occurs as a result of several relaxation mechanisms in the polymer. The core and shell nanoparticles with a specific thickness of shells, an unexpected dielectric behavior that strengthened EMI shielding effectiveness was demonstrated. On the other hand, Liu et al. presented the well-defined shells, unique morphological characteristics, desirable magnetization, large surface area, and large porosity of the yolk-double-shelled Fe_3O_4@SnO_2 particles significantly enhanced the EMI SE characteristics of the composite [161]. The significant increase in the absorption of EM wave of the composite containing Fe_3O_4@SnO_2 can be attributed to the individual shells in the yolk-shell structure, which provided the synergistic effect between the core containing magnetic Fe_3O_4 and the dielectric shell containing SnO_2 nanoparticles. Zhang et al. chose Polyaniline (PANI) and bagasse fiber (BF) to develop a heterostructure by insulating PANI over the fiber surface to form a conductive light weight material. The properties depend on the total coverage of PANI on the fiber surface as, higher the PANI content more the electrical conductivity. The material showed good complex permittivity because PANI improves dipolar polarization and conductivity. [81]

The exceptional EMI shielding properties of these nanoparticles were attributed to the complementary activity of the dielectric loss and the magnetic loss generated in the composite due to core-shell structure nanoparticles. Owing to the presence of the conductive shells or core, the eddy current effect was effectively minimized, and anisotropy energy was increased in the core-shell structured nanoparticles [162]. Owing to the presence of the magnetic core or shell, magnetic losses such as natural ferromagnetic resonance loss, domain wall resonance loss, and hysteresis loss are produced, which usually play an important role in the enhancement of EMI shielding effectiveness.

In overview, composites containing core@shell nanoparticles are receiving great attention due to their potential advantages such as core-corrosion safety, interfacial polarization, complementary behavior, and confinement effect. Furthermore, a wide range of composites containing core@shell nanoparticles with reasonable attenuation of EM waves have been investigated and data were listed in Table 8.

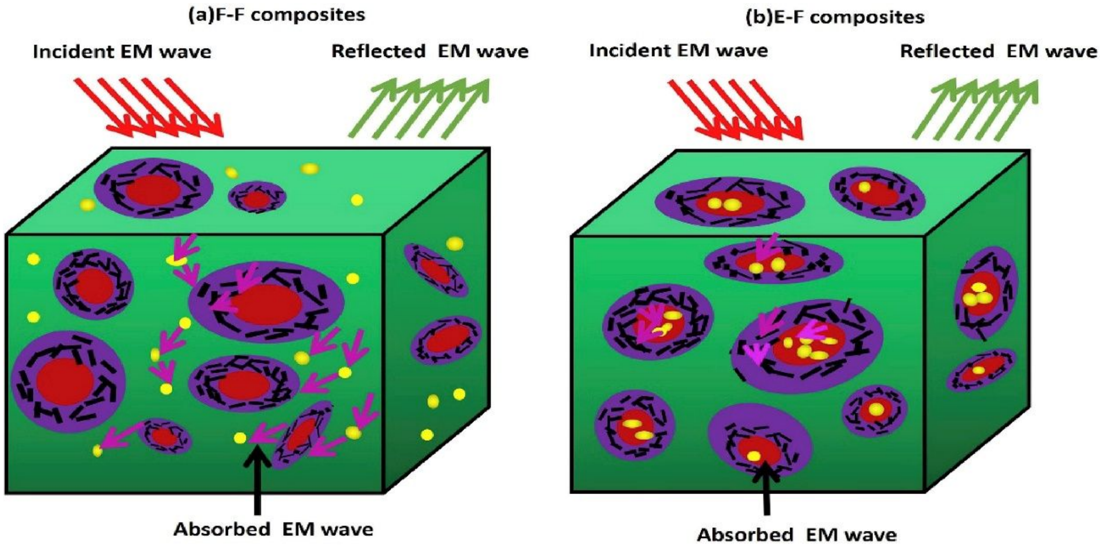

Fig.11: Cartoon illustrating the process of EMI shielding EMI shielding mechanism for the composites. Reprinted with permission. Copyright (2018) [163]

View Article Online
DOI: 10.1039/D4NA00572D

Table 8. Polymer composites containing core and shell particles and their EMI shielding effectiveness

Materials	Thickness (mm)	Conductivity (s/m)	EMI SE (dB)	Frequency (GHz)	Ref
PVDF/FeCoSiO2@MWNT (10 wt%)	3	-	35	2-18	[162]
Fe_3O_4@C@PANI (Fe_3O_4@ C:PANI::1:9)	1	4.06×10^{-1}	65	2-8	[164]
FeCo@SiO_2@ PPy	2.1	-	65.17	2-18	[165]
PVDF/F_3O_4(3 wt%)@SiO2@ MWCNTs(10 wt%)	0.6	2×10^{-3}	40	12-18	[166]
fMWCNT-Fe3O4@Ag/ epoxy (MWCNT: Fe3O4::9:1)	2	28	35	8.2-12.4	[167]
F_3O_4 (20 wt%) @SiO2@PPy	0.27	71	32	8-12.4	[168]
PVDF/PS/HDPE/MWCNTs(70/20/10/1vol%)	2.5	1.2	25	8-12.4	[163]
Ni@SnO2@PPy	3.5	14.28	30.1	2-18	[169]
Co@C-PVDF	-	-	25.49	8-12.4	[170]

View Article Online
DOI: 10.1039/D4NA00572D

3.8 Segregated structures

The conductive polymer composites were incorporated with large loadings of conductive fillers into the polymer matrix to form a percolated network structure which increases the electrical conductivity of the polymer composite. This conventional approach in the fabrication of polymer composite improves their density but is not a cost-effective or industrially viable method. Owing to such issues, the segregated structure facilitates the formation of percolated network with low filler loadings in the fabrication of polymer composites among all other structure-based strategies. Typically, two approaches are employed for developing segregated structures. One approach is the addition of conductive fillers to form a percolated network in the polymer matrix through the densification process. The conductive filler loadings in the segregated network structure resulted in a percolated conductive network structure integrated with the polymer matrix. Furthermore, the segregation of conductive fillers by distinct polymeric bulks improves the composite's EMI shielding performance. The other approach is to prefabricate 3D integrated conductive structures, and subsequently fill the pores with the polymer matrix. Li et al. presented a novel process for producing a segregated composite of poly(phenylene sulfide) (PPS) containing carbon nanotubes (CNT) [171]. Firstly, PPS beads were mechanically blended with CNT to produce PPS complex granules coated with CNT. Then was followed by compression molding into segregated composites of CNT/PPS. The EMI shielding effectiveness of the segregated composite of CNT/PPS was significantly higher than that of the random ones. Segregated structures were exhibiting excellent EMI shielding effectiveness [171]. Similarly, Yu et al. studied an electrostatic assembly method for producing highly conductive Polystyrene (PS) nanocomposites containing Mxene [172]. In this method, the negative MXene pre-coated on positive PS microspheres, followed by compression molding. The resulting PS composites containing MXene have a lower percolation threshold limit of 0.26 vol%, resulting in a good electrical conductivity of 1081 S/m and an excellent EMI SE of 54 dB over the X-band frequency range of 8-12.4 GHz [172]. Liang et al. developed a three-dimensional foam with systematic hollow spherical structures of reduced graphene oxide and silver platelets (rGO/AgP) [159]. By using a freeze-drying process, the foam composite accomplished a uniform distribution of AgP and rGO, forming a network structure. The final nanocomposites containing highly stable segregated structures were successfully fabricated by backfilling the epoxy monomer and curing agent. The 3D segregated structures of AgP/rGO/EP nanocomposites containing 0.44 vol% rGO and 0.94 vol% AgP showed the maximum SE_T value of 58 dB in the X-band frequency range of 8-12.4 GHz and electrical conductivity of 45.3 S/m due to systematic percolation networks of the AgP/rGO hollow spherical particles and the interfacial synergy between hollow spherical particles and epoxy resin [159]. Many authors have reported that the segregated structures in the literature used in the fabrication of EMI shielding materials were listed in Table 9.

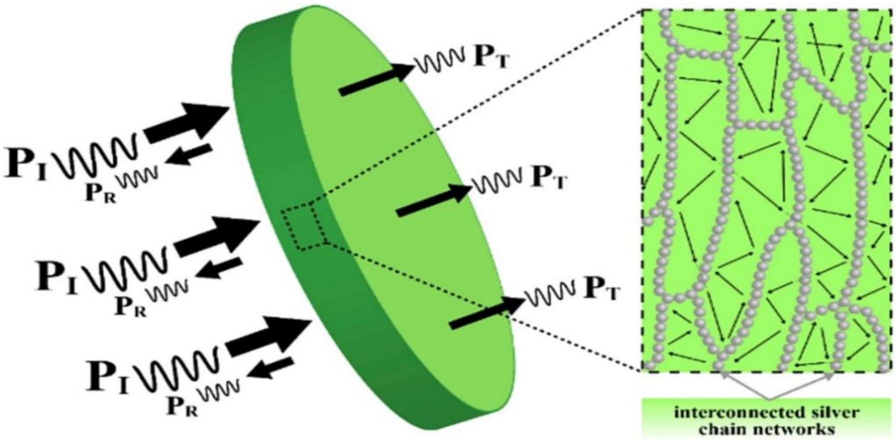

Fig.12: Schematic EMI shielding mechanism for the PLA/Ag composites with novel segregated electrically conductive Ag networks. Reprinted with permission. Copyright (2018) [173]

Table 9. Segregated structure composites and their EMI shielding effectiveness

Materials	Filler content	Thickness (mm)	Conductivity (s/m)	SE_T (dB)	Frequency (GHz)	Ref
PP/CNT/CB foam	5 wt%	0.26	6.67×10^{-1}	72.23	8.2-12.4	[174]
PS/MWNT	7 wt%	1.8	11	26.3	8.2-12.4	[175]
PDMS/MWNT/SGM	SGM-30vol%; MWNT-3vol%	2.7	50	55	8.2-12.4	[176]
PDMS/MWNT/HGM	HGM-40vol%; MWNT-3vol%	2.7	47.5	53	8.2-12.4	[176]
PMMA/rGO	2.6vol%	2.9	91.2	63.2	8.2-12.4	[177]
PMMA/rGO/magnetite	rGO-1.1vol% Magnetite-0.5 vol%	2.9	-	29	8.2-12.4	[177]
NR/Fe_3O_4@rGO	78% Fe_3O_4 10phr rGO	1.8	6.1	42.4	8.2-12.4	[178]
NR/rGO	10phr rGO	1.8	8.1	34	8.2-12.4	[178]
CNT/UHMWPE	4 wt%	2	30.1	32.6	8-18	[179]
PLA/Ag	5.89vol%	1.5	254	50	8.2-12.4	[180]
PVDF/MWNT	7 wt%	3	6	45	8.2-12.4	[181]
PLLA/MWNT	1.1 wt%	1.5	25	30	8.2-12.4	[182]

View Article Online
DOI: 10.1039/D4NA00572D

3.9 Template Structure

In the polymer composites, the addition of large filler loadings of nanomaterials in the polymer matrix attenuates EM waves. The addition of large filler loadings in the polymer matrix resulted in the formation of agglomerates and the dense stacking of polymers in the nanocomposite. In response to such problems, introducing 3D porous template structures will effectively overcome the agglomeration of nanomaterials. The major studies on template-based polymer composites and the researchers used templates to create 3D porous structures. Li et al. used a sacrificial template approach to build 3D foam structures with rGO and Mxene [183]. The template was produced from an Al_2O_3 honeycomb plate. MXene self-assembly on rGH resulted in honeycomb structural rGO-MXene (rGMH) with the formation of percolated networks and excellent EMI shielding properties. The honeycomb cell size of 0.5 mm contains 1.2 wt% of rGO and 3.3 wt% of MXene /epoxy nanocomposite demonstrating the electrical conductivity of 387.1 S/m and SE_T value of 55 dB values [183].

Recently, Shahzad et al. studied the renewable porous biochar and 2D MXene have sparked tremendous interest in high-performance EMI shielding fields due to their particular ordered structures and good electrical conductivity values [183]. The wood-based porous carbon from natural wood was used as a template in this study. The composites containing 15 wt% of MXene/ epoxy and 4.25 wt% of MXene foam/epoxy were prepared by direct blending and template methods corresponding to SE_T values of 41 and 46 dB, respectively. Many authors have reported the template-based structures in the literature for the fabrication of EMI shielding materials were listed in Table 10.

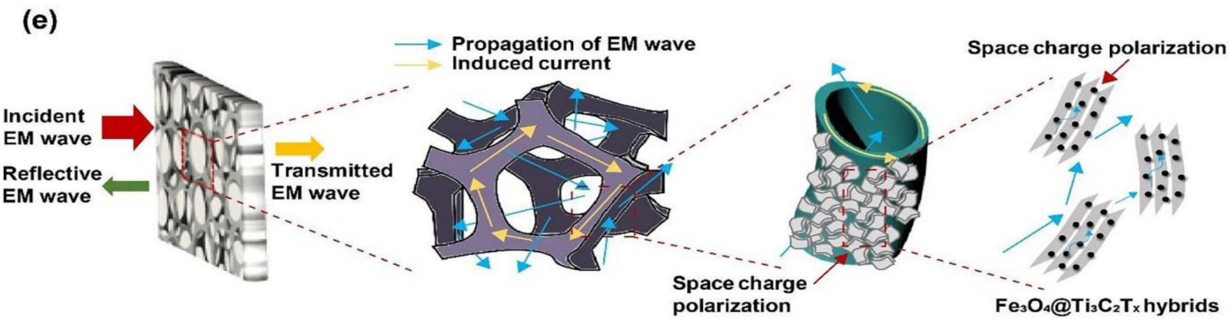

Fig.13: Schematic diagram of the EM waves absorption in Fe3O4@Ti3C2TX/GF/PDMS composite. Reprinted with permission. Copyright (2020) [184]

Table 10. The template-based structures for the fabrication of EMI shielding materials

Materials	Template	Conductivity (S/m)	SE_T (dB)	Frequency (GHz)	Ref
10.69 wt% Mxene (Ti_3C_2TX) /PDMS			30	8.2-12.4	[184]
10.69 wt% Graphene/PDMS			15	8.2-12.4	[184]
10.69 wt% MXene/11.53 wt% Fe_3O_4/graphene/PDMS	Graphene		80	8.2-12.4	[184]
10.69 wt% MXene/ 11.53 wt% Fe_3O_4 /graphene/PDMS	Graphene		77	26.5-40	[184]
1.2 wt% rGO/MXene/epoxy	Al_2O_3	36	43.5	8.2-12.4	[185]
3.3 wt% rGO/MXene/epoxy	Al_2O_3	387.1	55	8.2-12.4	[185]
12 wt% Graphene foam/hollow-Fe3O4/Polydimethylsiloxane	Nickel foam		70.37	8.2-12.4	[186]
2.76 wt% of Fe3O4 chemically bonded carbon nanotubes/ reduced graphene foams (RGF)/epoxy	RGF	7.3×10^{-5}	36	8.2-12.4	[187]
2.76 wt% of carbon nanotubes/reduced graphene foams/epoxy	RGF	14	31	8.2-12.4	[187]
2.58 wt% of PANI/0.83 wt% of MWCNT/1.20 wt% of thermally annealed graphene /epoxy	PANI	5210	42	8.2-12.4	[188]
1.5 wt% of Fe3O4/ 1.2 wt% of thermally annealed graphene oxide/epoxy	Graphene	8.7×10^{-5}	10	8.2-12.4	[189]
1.5 wt% of Fe3O4/ 1.2 wt% of thermally annealed graphene/epoxy	Graphene	27.5	35	8.2-12.4	[189]

View Article Online
DOI: 10.1039/D4NA00572D

4 Process-based strategies of nanomaterials for the fabrication of efficient EMI shielding materials

To develop EMI shielding materials, the homogenous distribution of nanomaterials in the polymeric matrix is a fundamental design strategy focused on delivering uniform dispersion of the incorporated fillers in the polymer. The nanomaterials in the polymer matrix combined to create a percolation network that relies on a filler loading of nanoparticles. Nevertheless, nanofillers have various sizes and multiple dimensions, and the filler loading of nanoparticles in large quantities makes them vulnerable to agglomeration in the polymer matrix, thereby significantly affecting the composites' performances [4]. The miscibility of nanoparticles may increase by introducing an external force. Melt blending, solvent mixing, and in situ polymerization are all approaches for achieving a homogeneous structure. Melt blending is an economically feasible, cost-effective, and realistic method in the polymer industry. In this method, the polymer matrix was heated at melting temperature rather than its solubility in conventional solvents, preventing the solvent removal stage [4].

The high-quality shear mixing method will ensure that the fillers are well dispersed in the molten polymer. Kumar et al. used a continuous melt blending technique to achieve homogeneous dispersion of large filler loadings of MWNT within a polypropylene (PP) polymeric matrix [11]. Morphological characteristics were analysed and confirms the good dispersion of MWNT in the nanocomposites. The nanocomposite with an MWNT loading of 2 wt% demonstrated an SE_T value of 5.9 dB, which corresponds to 74.29% attenuation of incident EM wave power over the X-Band frequency range of 8–12.4 GHz. Many authors have reported in the literature that the melt blending method used in the fabrication of EMI shielding materials was listed in Table 10.

Solution mixing depends on a solvent technique, which finely disperses the fillers in the matrix due to the polymer's lower viscosity. Because of the filler's limited solubility in the solvent, certain processing steps such as intense stirring, high-intensity ultrasonication, and surface modification are needed. Ouyang et al. produced an intrinsically conducting polymer composed of poly(3,4-ethylene dioxythiophene) (PEDOT) and polystyrene sulfonate (PSS) as a conductive portion for the development of highly effective flexible EMI materials [190]. PEDOT and PSS were mixed with an extremely stretchable, miscible

View Article Online
DOI: 10.1039/D4NA00572D

polyurethane (PU) solution to create composite films by drop-casting. The 0.15 mm thick films exhibited a conductivity of 7.7×10^3 S/m and demonstrated a SE_T value of 62 dB over the X-band frequency range of 8-12.4 GHz. In situ polymerization is a reasonably complex process in which the dispersion of the filler is timed to correspond with the matrix's polymerization. Zhang et al. generated a sequence of conductive polymeric composites by polymerizing ε-caprolactam monomer in situ in the presence of GO nanosheets in a single step [190]. The reduction, refinement, and distribution of GOs occurred by the polymerization, with no additional reducing agents utilized. In the in-situ polymerization process, epoxy-based composites were commonly used. The addition of the nanoparticles in the composite helped create conductive networks while also contributing to hysteresis degradation, resulting in significantly enhanced absorption of EM waves. It is believed that by using various processes, a higher efficient polymer composite containing filler loading of nanoparticles would be possible, which would be accomplished using processing techniques as listed in Table 11.

Table 11. Processing strategies used in the fabrication of efficient EMI shielding materials

Materials	Method	Conductivity (S/m)	SE_T (dB)	Frequency (GHz)	Ref
Fabrics/10 wt% CNT and sodium alginate	20 cycles of layer-by-layer assembly	36.6	21.5	8.2-12.4	[191]
Fabrics/10 wt% CNT and sodium alginate	20 cycles of layer-by-layer assembly	36.6	20.8	12.4-18	[191]
PS/5 wt%MWCNT	Nano-Infiltration	$7.2x10^{-2}$	25	8.2-12.4	[192]
PS/5 wt%MWCNT/rGO/Fe_3O_4	Nano-Infiltration	0.014	22	8.2-12.4	[192]
PS/5 wt%MWCNT/rGO/MoS2	Nano-Infiltration	0.031	36	8.2-12.4	[192]
PLA/30 wt% of PVDF/0.25 wt%of CNT	Kinetically controlled melt blending	1.06×10^{-2}	< 3.5	8.2-12.4	[193]
PLA/30 wt% of PVDF/0.25 wt%of CNT	Kinetically controlled melt blending	1.06×10^{-2}	< 8	1-6	[193]
20 vol% PS/PMMA /2.7 vol% MWNT	Intertube and interphase controlled melt blending	90	29-20	8.2-12.4	[194]
PDMS/3 wt% of MWNT	Spin coated	40	13.5	8.2-12.4	[195]
PDMS/3 wt% of MWNT	Compression molding	88	7	8.2-12.4	[195]
50 wt% PC/PMMA/3 wt% MWNT	Solution mixing	0.5	8-14	8-12	[196]
50 wt% PC/PMMA/3 wt% MWNT	Melt blend	0.3	4.5-9	8-12	[196]
0.5 wt % E-f-GO/epoxy/carbon fiber	VARTM technique	-	55-67	12.4-18	[197]
PVDF/30 wt% Ni	The rotational orientation of filler	-	20–35	26.5-40	[198]

7.5 wt% of (Graphene/MWNT)/PBO	Insitu polymerization		50.17	12.58	[199]
2 wt % Ionic Liquid-MWNT + 5 wt % BaFe in PC + 10 wt% PMMA	Melt blending	2.8	37	8-18	[200]
PET/PANI composite	in-situ chemical oxidation polymerization method	80	23.95	8-12.4	[201]
35 wt% of EVA/40 wt% of CF/5 wt% OMMT/20 wt% SCF	Ceramization	99	36	8-12.4	[202]
PS/12.6 vol% Cu	compression molding	2.95×10^6	100	0.1-18	[203]
PS/12.6 vol% Cu/0.4 vol% Ag	compression molding	3.5×10^6	110	0.1-18	[203]
PVDF/2 wt% MWNT	Extrusion followed rolling	2.8×10^{-3}	18-25	12-18	[204]
EMA/50 wt% of EOC/ 15 wt% of MWNT	Solution mixing	0.89	33	8-12.4	[205]
60 wt% of AEM/MPU/5 wt% of SWNT	Blending	4.27×10^{-2}	23-27	2-8	[206]
ABS/1.5 wt% of CNT /1.5 wt% of CB	Extrusion followed by vacuum drying	4.7×10^{-3}	11	8-12.4	[207]
ABS/3 wt% of CNT	Extrusion followed by vacuum drying	1.27×10^{-3}	17	8-12.4	[207]
40 wt% of CNT/PLA	Melt blending	3.2	50	8-12.4	[208]
40 wt% of CNT/PLA	3D printing	1.1	30	8-12.4	[208]
48 wt% of Poly(L-lactide)/12 wt% of Poly(ε-caprolactone)/PCL/2Carbon Nanotubes	Melt blending	0.012	17	8-12.4	[209]

View Article Online
DOI: 10.1039/D4NA00572D

5 Sustainable strategies of nanomaterials for the fabrication of efficient EMI shielding materials

A sustainable polymer is a plastic material that satisfies consumer demands without harming the environment, health, or economy. To accomplish this, scientists are focusing on creating polymers that, as compared to non-sustainable alternatives, use renewable feedstocks, such as plants, and crops for manufacturing with a smaller carbon footprint and a facile end life. Although sustainable polymers are a significant rising segment of the industry, they are derived from unsustainable fossil materials and require adequate synthesis and processing. A natural polymer, as a non-toxic, reusable, and renewable fuel, may be directly carbonized to produce macroscopic materials without the use of expensive precursors or complicated processes, implying an efficient energy-saving path for EMI shielding materials. As precursors, two prominent natural products, cellulose, and lignin have received considerable attention. Since graphene oxide can only be uniformly distributed in water at lower concentrations, the resulting graphene aerogels have low density, good mechanical strength, and conductivity. In contrast to graphene oxide, Zeng et al. discovered that lignin could form stable suspensions in a much wider range of concentrations, resulting in honeycomb-like foams with tunable densities through unidirectional freeze-drying [190]. As a result of their research, honeycomb-like lignin-derived carbon (LC) foams doped with rGO were created using unidirectional ice-templating, freeze-drying, and carbonization. The interfaces between the LC and rGO and the aligned pores in the 2 mm thick honeycomblike foams contributed interfacial polarization loss and numerous reflections, resulting in a Collection of 31 dB over the X-band frequency range of 8-12.4 GHz. Because of their broad specific area and porous nature, Wan et al. chose cellulose-derived carbon aerogels (CDCA) as materials [190]. Then, using a simple chemical precipitation process, nanoneedles and nanoflowers of magnetic α-FeOOH were developed in-situ on CDCA substrate to increase the contributions of magnetic losses and thus improve the EMI shielding characteristics. The incorporation of α-FeOOH into carbon aerogels exhibited an absorption-dominant mechanism, which certainly reduced secondary radiation from EMI shields as a prepared composite was a compelling option for designing safety devices from EM radiation. Furthermore, a volume of natural biomass rich in natural polymers, such as wood, straw, pulp, flour, cotton, and

View Article Online
DOI: 10.1039/D4NA00572D

sugarcane, has been used as a precursor, which has proven to be a potential candidate for application as EMI shielding material. Another area of importance should be recovering materials from electrical and electronic devices into matrix and reinforcement for EMI shielding applications leading to waste management and sustainability. Rosa et al. worked on using e-waste as metal fillers to the polymer matrix. The polymer matrix was High density polyethylene (HDPE) recovered from municipal solid waste. The metal filler, mostly iron oxide was separated from printed circuit boards (PCB), and the EMI SE was observed to be 48.3 dB. Rahaman et al. investigated recycling and reusing Polyethylene (PE) from waste plastic materials to be used as packaging for electronic devices. Carbon black was used as the conducting filler to improve the shielding property, and the composite showed an EMI SE value of 33 dB at a thickness of 1mm and an attenuation of 99.93%. [210], [211] Many authors have reported sustainable nanocomposites for EMI shielding purposes and are listed in Table 12.

Table 12. Sustainable nanocomposites used in the EMI shielding applications

Materials	Novelty	Filler content	Thickness (mm)	Conductivity (s/m)	EMI SE (dB)	Frequency (GHz)	Ref
PU/MWCNTs/Fe_3O_4@ MoS_2	Self-healing composites	3 wt% MWCNT; 5 wt% Fe_3O_4 @MoS_2	5	-	-36.6	8-18	[212]
MWCNTs/rGO/ Fe_3O_4/PU	Ultrafast Self-healing composites	3 wt% MWCNT; 5 wt% rGO/Fe_3O_4	5.8	0.05	-36	8-18	[213]
PU/MWCNTs/ rGO@MoS2@Fe3O4	Trigger free self-healing	3 wt% MWCNT; 5 wt% rGO@MoS2 @Fe3O4	5	10^{-1}	-43.6	8-18	[214]
GEs/CNTs/Elastomeric ionomers	Recyclable and Self-healing (100% recovery)	10 wt%	1	550	64	8.2-12.4	[215]
Fe_3O_4@MWCNTs/PAM	Recoverable and Self-healing	20 wt% Fe_3O_4@ MWCNTs	1.8	-	-50	8.2-12.4	[216]
MWCNT/Ni@CLF/PEEK	Renewable biomaterials	18 wt% Ni@CLF	2.5	2.101	48.1	8.2-12.4	[217]
PLLA/CPEGDA/MWCNT	Sustainable eco-friendly	3.6vol% MWCNT	1	10^{-1}	27.4	8.2-12.4	[218]
PLA/GNP	Naturally derived biodegradable nanocomposites	15 wt% GNP	2.5	7.4	15	8.2-12.4	[219]
PBAT/GNP	Naturally derived biodegradable nanocomposites	15 wt% GNP	2.5	3	14	8.2-12.4	[219]

PLA/Graphite foams	Renewable and biodegradable nanocomposites	2.5 wt%	2	3.5	45	8.2-12.4	[220]
PLA/Graphite solid	Renewable and biodegradable nanocomposites	2.5 wt%	2	2×10^{-6}	20	8.2-12.4	[220]
PLA/MWCNT foams	Biodegradable nanocomposites	0.0054vol% MWCNT	5	-	45	8.2-12.4	[221]
PLA/GNP	Biodegradable nanocomposites	15 wt% GNP	1.5	7.4	15.5	5.85–12.4	[222]
PLLA-MWCNT	Biodegradable nanocomposites	10 wt% MWCNT	2.5	3.4	23	8.2-12.48	[223]
PANI/CNF	Environment friendly and sustainable	50 wt%PANI and 50 wt% CNF	1	31.4	-23	8.2-12.4	[224]
Waste Paper/Ag-based ink	Waste Paper based composite	-	0.36	-	68	10.77-18	[225]
WTP/PVA Carbon Aerogel	Waste Tissue Paper based carbon absorbing composite	6 wt% Waste Tissue Paper	-	135	40	8.2-12.4	[226]
PVB-CoO_x-FAC	Usage of waste fly ash cenospheres	10 wt%	2.5	-	-27	15.8	[227]
PVB-NiO-FAC	Usage of waste fly ash cenospheres	10 wt%	2.5	-	-47.5	15.8	[227]
PVB-PANI-FAC	Usage of waste fly ash cenospheres	10vol% FAC; 30vol% PANI; 60vol% PVB	265±2 μm	11	15	5.8-12.4	[228]

PVB-PANI-Ni-FAC	Usage of waste fly ash censopheres	10vol% Ni-FAC; 30vol% PANI; 60vol% PVB	259±2 μm	18S/m	23±1	5.8-12.4	[228]
PVB-PANI-Co-FAC	Usage of waste fly ash cenospheres	10vol% Co-FAC; 30vol% PANI; 60vol% PVB	261±2 μm	21S/m	19	5.8-12.4	[228]
$BC/Cu/Al_2O_3$	Usage of bacterial cellulose	-	-	0.69×10^{-12} S/m	65.3	1.5	[229]
PP/rGO	Usage of Vitamin C for in situ reduction of rGO	20 wt% rGO	2	10^{-1}S/m	50	8-18	[230]

View Article Online
DOI: 10.1039/D4NA00572D

6 Summary and perspective

Electromagnetic interference (EMI) has evolved as a result of rapid advances in the sectors of electronics and communications, offering a great opportunity for the development of efficient EMI shielding materials. Over continuous exploratory effort, polymer composites comprising conductive, magnetic, and/or dielectric materials as important constituents for preventing electromagnetic interference (EMI) are reported. Several processing techniques for the preparation of EMI shielding materials were discussed in this review. The structural design of nanofillers is critical and challenging work in the fabrication of EMI shielding materials, which integrates the functional filler with the polymer matrix for superior EMI shielding performance. Firstly, the role of basic nanofiller in the preparation of high-performance EMI shielding composites is outlined, along with preparation techniques and typical cases. Also, different-structured nanofillers are used simultaneously during the fabrication process to improve shielding performance was discussed. Secondly, the importance of the fabrication process for developing EMI shielding materials was summarized. In addition, different manufacturing strategies for lightweight and ultra-thin materials were addressed in order to be used as potential EMI shielding materials. Synthetic and natural polymers have been processed into various derivatives using facile synthesis processes that demonstrate significant promise for adequate preparations of EMI shielding materials. Furthermore, simple, large-scale, and low-cost fabrication methods for EMI shielding material for efficient industrialization and emerging structures were explored, as should the translation of corresponding shielding devices for potential applications. Finally, EMI shielding material fabrication techniques endow the EMI shields with unique properties, transforming them into high-value-added EMI shielding materials.

View Article Online
DOI: 10.1039/D4NA00572D

Nomenclature:

ABS: Acrylonitrile-butadiene-styrene

AEM: Ethylene acrylic elastomers

AIBN: Azoisobutyronitrile

Ag: Silver nanoparticles

Ag@HGM: Silver nanoparticles on the surface of hollow glass microspheres

BC: Bacterial cellulose

BN: Boron nitride

BNSF: $BaNd_{0.2}Sm_{0.2}Fe_{11.6}O_{19}$

BRF: polypyrrole matrix encapsulated with BST, RGO and Fe_3O_4

BST: Barium strontium titanate

CB: Carbon black

CCTO: $CaCu_3Ti_4O_{12}$

CDCA: Cellulose-derived carbon aerogels

CF: Carbon fibre

CLF: Carbonized loofah fiber

CNF: Cellulose nanofiber

CNT: Carbon nanotubes

CPEGDA: Crosslinked poly (ethylene glycol) diacrylate

CSA: Camphor sulfonic acid

EM: Electro-magnetic

EMA: Ethylene-co-methyl acrylate

EMI: Electro-magnetic Interference

EMI SE: Electro-magnetic Interference shielding effectiveness

View Article Online
DOI: 10.1039/D4NA00572D

EOC: Ethylene octene copolymer

FAC: Fly ash cenosphere

f-MWCNT: Functionalized Multiwalled Carbon Nanotubes

GFBT: Graphene nanoplate/ Fe_3O_4@$BaTiO_3$ hybrid

GN: Graphene nanosheets

GN-CN: graphene nanoplates-carbon nanotubes

GNP: Graphene nanoplatelets

HDPE: High density polyethylene

HGM: hollow glass microspheres

IL-MWCNT: Ionic Liquid- Multiwalled Carbon Nanotubes

Lbl: Layer-by-layer

LC: Lignin-derived carbon

MA: Maleic anhydride

MNP: Metal nanoparticles

MPU: Mill able polyurethane

MWNT or MWCNT: Multi-walled carbon nanotubes

NCF: Nickel doped cobalt ferrites

NF: Nonwoven fabric

Ni@CNT: Carbon nanotubes encapsulated nickel nanowires

NR: Natural Rubber

NWF: Non-woven fabrics

PAM: Polyazomethine

PANI: Polyaniline

PBAT: Poly (butylene adipate-co-terephthalate)

View Article Online
DOI: 10.1039/D4NA00572D

PBO: Poly(p- phenylenebenzobisoxazole)

PC: Polycarbonate

PCL: Polycaprolactone

PDMS: Polydimethylsiloxane

PEDOT: Poly(3,4-ethylene dioxythiophene)

PEEK: Polyether ether ketone

PET: Polyethylene terephthalate

PET Oxide: Poly (ethylene oxide)

PHDDT: Phosphorus-containing liquid crystalline co-polyester

P_I: Power density of incident electromagnetic waves

PLA: Poly (lactic acid)

PLLA: Poly(l-lactide)

PMMA: Poly (methyl methacrylate)

PNC: Polymer nanocomposites

POE: Poly(ethylene-co-1-octene)

PP: Polypropylene

PPy: Polypyrrole

PPEK: Poly (phthalazinone etherketone)

PPS: Poly (phenylene sulphide)

P_R: Power density of reflected electromagnetic waves

PS: Polystyrene

PSS: Polystyrene sulfonate

P_T: Power density of transmitted electromagnetic waves

p-TSA: para-Toluene Sulphonic Acid

View Article Online
DOI: 10.1039/D4NA00572D

PVA: Polyvinyl Alcohol

PVB: Poly (vinyl butyral)

PVDF: Polyvinylidene fluoride

RG-CN: Chemically reduced graphene oxide-carbon nanotubes

rGH: Honeycomb structural rGO

rGMH: Honeycomb structural rGO-MXene

RGO: Reduced graphene oxide

SBR: Styrene-butadiene rubber

SCF: Short carbon fiber

SE_A : EMI shielding effectiveness due to absorption loss

SE_R : EMI shielding effectiveness due to reflection loss

SE_T : Total EMI shielding effectiveness

SGM: Solid glass microspheres

SSE: Specific shielding effectiveness

SSF: Stainless steel fibre

Sub-SF: Substituted strontium ferrite

SWNT: Single-walled carbon nanotube

TAGA: Thermally annealed graphene aerogel

TGO: Thermally reduced graphene oxide

TGO-CN: Thermally reduced graphene oxide-carbon nanotubes

TPU: Thermoplastic polyurethane

UHMWPE: Ultrahigh-molecular-weight polyethylene

WPU: Waterborne polyurethane

View Article Online
DOI: 10.1039/D4NA00572D

WTP: Wastepaper

Conflicts of Interest

All authors declare that they have no conflicts of interest.

Data Availability

No primary research results, software or code have been included and no new data were generated or analysed as part of this review

References

[1] S. Sankaran, K. Deshmukh, M. B. Ahamed, and S. K. Khadheer Pasha, "Recent advances in electromagnetic interference shielding properties of metal and carbon filler reinforced flexible polymer composites: A review," *Compos. Part A Appl. Sci. Manuf.*, vol. 114, no. August, pp. 49–71, 2018, doi: 10.1016/j.compositesa.2018.08.006.

[2] X. C. Tong, "Advanced materials and design for electromagnetic interference shielding text book,2009."

[3] Paul and Clayton R, *Introduction to Electromagnetic Compatibility {Wiley Series in Microwave and Optical Engineering; 2nd Ed.}*. 2006.

[4] K. Bhaskaran, R. K. Bheema, and K. C. Etika, "The influence of Fe3O4@GNP hybrids on enhancing the EMI shielding effectiveness of epoxy composites in the X-band," *Synth. Met.*, vol. 265, no. May, 2020, doi: 10.1016/j.synthmet.2020.116374.

[5] V. Uma Varun, B. Rajesh Kumar, and K. C. Etika, "Hybrid polymer nanocomposites as EMI shielding materials in the X-band," *Mater. Today Proc.*, vol. 28, pp. 796–798, 2019, doi: 10.1016/j.matpr.2019.12.300.

[6] B. Rajesh Kumar and K. C. Etika, "Facile One-Pot Hydrothermal Synthesis of Copper Nanowires and Their Impact on the EMI Shielding Capability of Epoxy Composites," *Chem. Eng. Technol.*, vol. 45, no. 3, pp. 410–416, 2022, doi: 10.1002/ceat.202100389.

[7] R. K. Bheema, A. K. Ojha, A. V. Praveen Kumar, and K. C. Etika, "Synergistic influence of barium hexaferrite nanoparticles for enhancing the EMI shielding

performance of GNP/epoxy nanocomposites," *J. Mater. Sci.*, vol. 57, no. 19, pp. 8714–8726, 2022, doi: 10.1007/s10853-022-07214-8.

[8] S. Liu, S. Qin, Y. Jiang, P. Song, and H. Wang, "Lightweight high-performance carbon-polymer nanocomposites for electromagnetic interference shielding," *Compos. Part A Appl. Sci. Manuf.*, vol. 145, no. March, p. 106376, 2021, doi: 10.1016/j.compositesa.2021.106376.

[9] A. K. Singh, A. Shishkin, T. Koppel, and N. Gupta, "A review of porous lightweight composite materials for electromagnetic interference shielding," *Compos. Part B Eng.*, vol. 149, no. May, pp. 188–197, 2018, doi: 10.1016/j.compositesb.2018.05.027.

[10] L. Wang, Z. Ma, Y. Zhang, L. Chen, D. Cao, and J. Gu, "Polymer-based EMI shielding composites with 3D conductive networks: A mini-review," *SusMat*, vol. 1, no. 3, pp. 413–431, 2021, doi: 10.1002/sus2.21.

[11] R. Kumar, K. Kumar, N. Etakula, and K. C. Etika, "Enhanced thermo-mechanical , thermal and EMI shielding properties of MWNT / MAgPP / PP nanocomposites prepared by extrusion," *Compos. Part C Open Access*, vol. 4, no. December 2020, p. 100086, 2021, doi: 10.1016/j.jcomc.2020.100086.

[12] R. Turczyn, K. Krukiewicz, A. Katunin, J. Sroka, and P. Sul, "Fabrication and application of electrically conducting composites for electromagnetic interference shielding of remotely piloted aircraft systems," *Compos. Struct.*, vol. 232, no. October 2019, 2020, doi: 10.1016/j.compstruct.2019.111498.

[13] H. K. Choudhary, R. Kumar, S. P. Pawar, S. Bose, and B. Sahoo, "Effect of Microstructure and Magnetic Properties of Ba-Pb-Hexaferrite Particles on EMI Shielding Behavior of Ba-Pb-Hexaferrite-Polyaniline-Wax Nanocomposites," *J. Electron. Mater.*, vol. 49, no. 3, pp. 1618–1629, 2020, doi: 10.1007/s11664-019-07478-y.

[14] B. Zhang, J. Wang, J. Wang, H. Duan, S. Huo, and Y. Tang, "Coprecipitation synthesis of hollow poly(acrylonitrile) microspheres@$CoFe_2O_4$ with graphene as lightweight microwave absorber," *J. Mater. Sci. Mater. Electron.*, vol. 28, no. 4, pp. 3337–3348, 2017, doi: 10.1007/s10854-016-5927-x.

[15] T. Su, B. Zhao, F. Han, B. Fan, and R. Zhang, "The effect of hydrothermal temperature on the crystallographic phase of MnO_2 and their microwave absorption properties," *J. Mater. Sci. Mater. Electron.*, vol. 30, no. 1, pp. 475–484,

2019, doi: 10.1007/s10854-018-0312-6.

[16] B. Zhang *et al.*, "Double-shell PANS@PANI@Ag hollow microspheres and graphene dispersed in epoxy with enhanced microwave absorption," *J. Mater. Sci. Mater. Electron.*, vol. 30, no. 10, pp. 9785–9797, 2019, doi: 10.1007/s10854-019-01315-y.

[17] M. K. Naidu, K. Ramji, B. V. S. R. N. Santhosi, K. Krushna Murthy, C. Subrahmanyam, and B. Satyanarayana, "Influence of NiFe Alloy Nanopowder on Electromagnetic and Microwave Absorption Properties of MWCNT/Epoxy Composite," *Adv. Polym. Technol.*, vol. 37, no. 2, pp. 622–628, 2018, doi: 10.1002/adv.21703.

[18] M. K. Vyas and A. Chandra, "Synergistic effect of conducting and insulating fillers in polymer nanocomposite films for attenuation of X-band," *J. Mater. Sci.*, vol. 54, no. 2, pp. 1304–1325, 2019, doi: 10.1007/s10853-018-2894-z.

[19] L. Liu *et al.*, "Electromagnetic response of magnetic graphene hybrid fillers and their evolutionary behaviors," *J. Mater. Sci. Mater. Electron.*, vol. 27, no. 3, pp. 2760–2772, 2016, doi: 10.1007/s10854-015-4088-7.

[20] X. S. Hu, Y. Shen, L. S. Lu, J. Xu, and J. J. Zhen, "Enhanced electromagnetic interference shielding effectiveness of ternary PANI/CuS/RGO composites," *J. Mater. Sci. Mater. Electron.*, vol. 28, no. 9, pp. 6865–6872, 2017, doi: 10.1007/s10854-017-6386-8.

[21] H. Lu *et al.*, "Electromagnetic shielding of ultrathin, lightweight and strong nonwoven composites decorated by a bandage-style interlaced layer electropolymerized with polyaniline," *J. Mater. Sci. Mater. Electron.*, vol. 30, no. 23, pp. 20420–20431, 2019, doi: 10.1007/s10854-019-02379-6.

[22] G. Sun, H. Wu, Q. Liao, and Y. Zhang, "Enhanced microwave absorption performance of highly dispersed CoNi nanostructures arrayed on graphene," *Nano Res.*, vol. 11, no. 5, pp. 2689–2704, 2018, doi: 10.1007/s12274-017-1899-2.

[23] M. P. Gashti, S. T. Ghehi, S. V. Arekhloo, A. Mirsmaeeli, and A. Kiumarsi, "Electromagnetic shielding response of UV-induced polypyrrole/silver coated wool," *Fibers Polym.*, vol. 16, no. 3, pp. 585–592, 2015, doi: 10.1007/s12221-015-0585-9.

[24] D. Jiang *et al.*, "Electromagnetic Interference Shielding Polymers and Nanocomposites - A Review," *Polym. Rev.*, vol. 59, no. 2, pp. 280–337, 2019, doi:

View Article Online
DOI: 10.1039/D4NA00572D

10.1080/15583724.2018.1546737.

[25] K. Müller *et al.*, "Microwave Absorption and EMI Shielding Behavior of Nanocomposites Based on Intrinsically Conducting Polymers, Graphene and Carbon Nanotubes," *Carbon N. Y.*, vol. 4, no. 1, pp. 371–375, 2014, doi: 10.5772/48779.

[26] N. Maruthi, M. Faisal, and N. Raghavendra, "Conducting polymer based composites as efficient EMI shielding materials: A comprehensive review and future prospects," *Synth. Met.*, vol. 272, no. October 2020, p. 116664, 2021, doi: 10.1016/j.synthmet.2020.116664.

[27] M. Z. Rong, M. Q. Zhang, Y. X. Zheng, H. M. Zeng, R. Walter, and K. Friedrich, "Structure-property relationships of irradiation grafted nano-inorganic particle filled polypropylene composites," *Polymer (Guildf).*, vol. 42, no. 1, pp. 167–183, 2001, doi: 10.1016/S0032-3861(00)00325-6.

[28] F. P. Du *et al.*, "PEDOT:PSS/graphene quantum dots films with enhanced thermoelectric properties via strong interfacial interaction and phase separation," *Sci. Rep.*, vol. 8, no. 1, pp. 1–12, 2018, doi: 10.1038/s41598-018-24632-4.

[29] J. B. Hooper and K. S. Schweizer, "Theory of phase separation in polymer nanocomposites," *Macromolecules*, vol. 39, no. 15, pp. 5133–5142, 2006, doi: 10.1021/ma060577m.

[30] H. Xia and M. Song, "Preparation and characterization of polyurethane-carbon nanotube composites," *Soft Matter*, vol. 1, no. 5, pp. 386–394, 2005, doi: 10.1039/b509038e.

[31] Z. Zeng, H. Jin, M. Chen, W. Li, L. Zhou, and Z. Zhang, "Lightweight and Anisotropic Porous MWCNT/WPU Composites for Ultrahigh Performance Electromagnetic Interference Shielding," *Adv. Funct. Mater.*, vol. 26, no. 2, pp. 303–310, 2016, doi: 10.1002/adfm.201503579.

[32] Y. Zhang, T. Pan, and Z. Yang, "Flexible polyethylene terephthalate/polyaniline composite paper with bending durability and effective electromagnetic shielding performance," *Chem. Eng. J.*, vol. 389, no. February, p. 124433, 2020, doi: 10.1016/j.cej.2020.124433.

[33] K. Bhaskaran, R. K. Bheema, K. C. Etika, B. Krithika, B. R. Kumar, and K. C. Etika, "The influence of Fe3O4@GNP hybrids on enhancing the EMI shielding

effectiveness of epoxy composites in the X-band," *Synth. Met.*, vol. 265, no. March, 2020, doi: 10.1016/j.synthmet.2020.116374.

[34] Y. Liu, D. Song, C. Wu, and J. Leng, "EMI shielding performance of nanocomposites with MWCNTs, nanosized Fe 3O4 and Fe," *Compos. Part B Eng.*, vol. 63, pp. 34–40, 2014, doi: 10.1016/j.compositesb.2014.03.014.

[35] H. Jia *et al.*, "3D graphene/ carbon nanotubes/ polydimethylsiloxane composites as high-performance electromagnetic shielding material in X-band," *Compos. Part A Appl. Sci. Manuf.*, vol. 129, no. November 2019, p. 105712, 2020, doi: 10.1016/j.compositesa.2019.105712.

[36] K. Yu *et al.*, "RGO/Fe3O4 hybrid induced ultra-efficient EMI shielding performance of phenolic-based carbon foam," *RSC Adv.*, vol. 9, no. 36, pp. 20643–20651, 2019, doi: 10.1039/c9ra04244j.

[37] N. Bagotia, V. Choudhary, and D. K. Sharma, *Synergistic effect of graphene/multiwalled carbon nanotube hybrid fillers on mechanical, electrical and EMI shielding properties of polycarbonate/ethylene methyl acrylate nanocomposites*, vol. 159. Elsevier Ltd, 2019.

[38] H. Liu *et al.*, "Novel 3D network porous graphene nanoplatelets /Fe3O4/epoxy nanocomposites with enhanced electromagnetic interference shielding efficiency," *Compos. Sci. Technol.*, vol. 169, no. October 2018, pp. 103–109, 2019, doi: 10.1016/j.compscitech.2018.11.005.

[39] M. Bayat, H. Yang, F. K. Ko, D. Michelson, and A. Mei, "Electromagnetic interference shielding effectiveness of hybrid multifunctional Fe3O4/carbon nanofiber composite," *Polymer (Guildf).*, vol. 55, no. 3, pp. 936–943, 2014, doi: 10.1016/j.polymer.2013.12.042.

[40] Y. Zhan *et al.*, "Fabrication of a flexible electromagnetic interference shielding Fe3O4@reduced graphene oxide/natural rubber composite with segregated network," *Chem. Eng. J.*, vol. 344, no. October 2017, pp. 184–193, 2018, doi: 10.1016/j.cej.2018.03.085.

[41] Y. Bhattacharjee and S. Bose, "Core-Shell Nanomaterials for Microwave Absorption and Electromagnetic Interference Shielding: A Review," *ACS Appl. Nano Mater.*, no. February, 2021, doi: 10.1021/acsanm.1c00278.

[42] S. K. Singh, M. J. Akhtar, and K. K. Kar, "Hierarchical Carbon Nanotube-Coated

DOI: 10.1039/D4NA00572D

Carbon Fiber: Ultra Lightweight, Thin, and Highly Efficient Microwave Absorber," *ACS Appl. Mater. Interfaces*, vol. 10, no. 29, pp. 24816–24828, 2018, doi: 10.1021/acsami.8b06673.

[43] J. Chen, J. Wu, H. Ge, D. Zhao, C. Liu, and X. Hong, "Reduced graphene oxide deposited carbon fiber reinforced polymer composites for electromagnetic interference shielding," *Compos. Part A Appl. Sci. Manuf.*, vol. 82, pp. 141–150, 2016, doi: 10.1016/j.compositesa.2015.12.008.

[44] M. Verma, S. S. Chauhan, S. K. Dhawan, and V. Choudhary, "Graphene nanoplatelets/carbon nanotubes/polyurethane composites as efficient shield against electromagnetic polluting radiations," *Compos. Part B Eng.*, vol. 120, pp. 118–127, 2017, doi: 10.1016/j.compositesb.2017.03.068.

[45] C. Liu, X. Ye, X. Wang, X. Liao, X. Huang, and B. Shi, "Collagen Fiber Membrane as an Absorptive Substrate to Coat with Carbon Nanotubes-Encapsulated Metal Nanoparticles for Lightweight, Wearable, and Absorption-Dominated Shielding Membrane," *Ind. Eng. Chem. Res.*, vol. 56, no. 30, pp. 8553–8562, 2017, doi: 10.1021/acs.iecr.7b01930.

[46] S. Shajari, M. Arjmand, S. P. Pawar, U. Sundararaj, and L. J. Sudak, "Synergistic effect of hybrid stainless steel fiber and carbon nanotube on mechanical properties and electromagnetic interference shielding of polypropylene nanocomposites," *Compos. Part B Eng.*, vol. 165, pp. 662–670, 2019, doi: 10.1016/j.compositesb.2019.02.044.

[47] A. H. A. Hoseini, M. Arjmand, U. Sundararaj, and M. Trifkovic, "Significance of interfacial interaction and agglomerates on electrical properties of polymer-carbon nanotube nanocomposites," *Mater. Des.*, vol. 125, no. April, pp. 126–134, 2017, doi: 10.1016/j.matdes.2017.04.004.

[48] P. Saini, V. Choudhary, B. P. Singh, R. B. Mathur, and S. K. Dhawan, "Polyaniline-MWCNT nanocomposites for microwave absorption and EMI shielding," *Mater. Chem. Phys.*, vol. 113, no. 2–3, pp. 919–926, 2009, doi: 10.1016/j.matchemphys.2008.08.065.

[49] J. M. Thomassin, C. Pagnoulle, L. Bednarz, I. Huynen, R. Jerome, and C. Detrembleur, "Foams of polycaprolactone/MWNT nanocomposites for efficient EMI reduction," *J. Mater. Chem.*, vol. 18, no. 7, pp. 792–796, 2008, doi:

10.1039/b709864b.

[50] X. Yang *et al.*, "Synchronously improved electromagnetic interference shielding and thermal conductivity for epoxy nanocomposites by constructing 3D copper nanowires/thermally annealed graphene aerogel framework," *Compos. Part A Appl. Sci. Manuf.*, vol. 128, no. October 2019, p. 105670, 2020, doi: 10.1016/j.compositesa.2019.105670.

[51] X. Zhao, W. Xu, W. Yi, and Y. Peng, "A flexible and highly pressure-sensitive PDMS sponge based on silver nanoparticles decorated reduced graphene oxide composite," *Sensors Actuators, A Phys.*, vol. 291, pp. 23–31, 2019, doi: 10.1016/j.sna.2019.03.038.

[52] S. Zeng *et al.*, "Flexible PVDF/CNTs/Ni@CNTs composite films possessing excellent electromagnetic interference shielding and mechanical properties under heat treatment," *Carbon N. Y.*, vol. 155, pp. 34–43, 2019, doi: 10.1016/j.carbon.2019.08.024.

[53] P. Xu, X. Han, J. Jiang, X. Wang, X. Li, and A. Wen, "Synthesis and characterization of novel coralloid polyaniline/BaFe 12O19 nanocomposites," *J. Phys. Chem. C*, vol. 111, no. 34, pp. 12603–12608, 2007, doi: 10.1021/jp073872x.

[54] W. Wang, S. P. Gumfekar, Q. Jiao, and B. Zhao, "Ferrite-grafted polyaniline nanofibers as electromagnetic shielding materials," *J. Mater. Chem. C*, vol. 1, no. 16, pp. 2851–2859, 2013, doi: 10.1039/c3tc00757j.

[55] S. Zhang, Y. Wang, Q. Ran, Q. Fu, and Y. Gu, "Electromagnetic interference shielding property of polybenzoxazine/graphene/nickel composites," *React. Funct. Polym.*, vol. 143, no. April, 2019, doi: 10.1016/j.reactfunctpolym.2019.104324.

[56] I. Arief, S. Biswas, and S. Bose, "FeCo-Anchored Reduced Graphene Oxide Framework-Based Soft Composites Containing Carbon Nanotubes as Highly Efficient Microwave Absorbers with Excellent Heat Dissipation Ability," *ACS Appl. Mater. Interfaces*, vol. 9, no. 22, pp. 19202–19214, 2017, doi: 10.1021/acsami.7b04053.

[57] S. Gao, S. H. Yang, H. Y. Wang, G. S. Wang, and P. G. Yin, "Excellent electromagnetic wave absorbing properties of two-dimensional carbon-based nanocomposite supported by transition metal carbides Fe3C," *Carbon N. Y.*, vol. 162, pp. 438–444, 2020, doi: 10.1016/j.carbon.2020.02.031.

[58] A. A. Al-Ghamdi *et al.*, "Conductive carbon black/magnetite hybrid fillers in

microwave absorbing composites based on natural rubber," *Compos. Part B Eng.*, vol. 96, pp. 231–241, 2016, doi: 10.1016/j.compositesb.2016.04.039.

[59] S. Biswas, I. Arief, S. S. Panja, and S. Bose, "Electromagnetic screening in soft conducting composite-containing ferrites: The key role of size and shape anisotropy," *Mater. Chem. Front.*, vol. 1, no. 12, pp. 2574–2589, 2017, doi: 10.1039/c7qm00305f.

[60] S. Biswas, S. S. Panja, and S. Bose, "Physical Insight into the Mechanism of Electromagnetic Shielding in Polymer Nanocomposites Containing Multiwalled Carbon Nanotubes and Inverse-Spinel Ferrites," *J. Phys. Chem. C*, vol. 122, no. 34, pp. 19425–19437, 2018, doi: 10.1021/acs.jpcc.8b05867.

[61] G. Sang *et al.*, "Electromagnetic interference shielding performance of polyurethane composites: A comparative study of GNs-IL/Fe 3 O 4 and MWCNTs-IL/Fe 3 O 4 hybrid fillers," *Compos. Part B Eng.*, vol. 164, no. January, pp. 467–475, 2019, doi: 10.1016/j.compositesb.2019.01.062.

[62] H. Cheng *et al.*, "Synergetic effect of Fe 3 O 4 nanoparticles and carbon on flexible poly (vinylidence fluoride) based films with higher heat dissipation to improve electromagnetic shielding," *Compos. Part A Appl. Sci. Manuf.*, vol. 121, pp. 139–148, 2019, doi: 10.1016/j.compositesa.2019.03.019.

[63] S. P. Pawar, M. Gandi, and S. Bose, "High performance electromagnetic wave absorbers derived from PC/SAN blends containing multiwall carbon nanotubes and Fe3O4 decorated onto graphene oxide sheets," *RSC Adv.*, vol. 6, no. 44, pp. 37633–37645, 2016, doi: 10.1039/c5ra25435c.

[64] J. Wu, Z. Ye, H. Ge, J. Chen, W. Liu, and Z. Liu, "Modified carbon fiber/magnetic graphene/epoxy composites with synergistic effect for electromagnetic interference shielding over broad frequency band," *J. Colloid Interface Sci.*, vol. 506, pp. 217–226, 2017, doi: 10.1016/j.jcis.2017.07.020.

[65] K. Sushmita, A. V. Menon, S. Sharma, A. C. Abhyankar, G. Madras, and S. Bose, "Mechanistic Insight into the Nature of Dopants in Graphene Derivatives Influencing Electromagnetic Interference Shielding Properties in Hybrid Polymer Nanocomposites," *J. Phys. Chem. C*, vol. 123, no. 4, pp. 2579–2590, 2019, doi: 10.1021/acs.jpcc.8b10999.

[66] W. C. Yu *et al.*, "Superior and highly absorbed electromagnetic interference

shielding performance achieved by designing the reflection-absorption-integrated shielding compartment with conductive wall and lossy core," *Chem. Eng. J.*, vol. 393, p. 124644, 2020, doi: 10.1016/j.cej.2020.124644.

[67] R. S. Yadav *et al.*, "Lightweight NiFe2O4-Reduced Graphene Oxide-Elastomer Nanocomposite flexible sheet for electromagnetic interference shielding application," *Compos. Part B Eng.*, vol. 166, pp. 95–111, 2019, doi: 10.1016/j.compositesb.2018.11.069.

[68] G. Datt, C. Kotabage, and A. C. Abhyankar, "Ferromagnetic resonance of NiCoFe2O4 nanoparticles and microwave absorption properties of flexible NiCoFe2O4-carbon black/poly(vinyl alcohol) composites," *Phys. Chem. Chem. Phys.*, vol. 19, no. 31, pp. 20699–20712, 2017, doi: 10.1039/c7cp03953k.

[69] A. Kobyliukh, K. Olszowska, U. Szeluga, and S. Pusz, "Iron oxides/graphene hybrid structures – Preparation, modification, and application as fillers of polymer composites," *Adv. Colloid Interface Sci.*, vol. 285, p. 102285, 2020, doi: 10.1016/j.cis.2020.102285.

[70] X. Li, Z. Sun, Y. Zhang, D. Huang, and J. Hu, "Effects of oxygen vacancies on dielectric properties and relaxor behavior of Ba(ZrxTi1-x)O3 ceramics," *J. Phys. Conf. Ser.*, vol. 2101, no. 1, 2021, doi: 10.1088/1742-6596/2101/1/012050.

[71] E. Cockayne, "Influence of oxygen vacancies on the dielectric properties of hafnia: First-principles calculations," *Phys. Rev. B - Condens. Matter Mater. Phys.*, vol. 75, no. 9, pp. 1–8, 2007, doi: 10.1103/PhysRevB.75.094103.

[72] B. K. Sahu and A. Das, "Significance of in-plane oxygen vacancy rich non-stoichiometric layer towards unusual high dielectric constant in nano-structured SnO2," *Phys. E Low-Dimensional Syst. Nanostructures*, vol. 103, no. February, pp. 60–65, 2018, doi: 10.1016/j.physe.2018.05.016.

[73] M. D. Li *et al.*, "Oxygen-vacancy-related dielectric relaxation behaviours and impedance spectroscopy of Bi(Mg1/2Ti1/2)O3 modified BaTiO3 ferroelectric ceramics," *J. Mater.*, vol. 4, no. 3, pp. 194–201, 2018, doi: 10.1016/j.jmat.2018.03.001.

[74] S. Biswas, Y. Bhattacharjee, S. S. Panja, and S. Bose, "Graphene oxide co-doped with dielectric and magnetic phases as an electromagnetic wave suppressor," *Mater. Chem. Front.*, vol. 1, no. 6, pp. 1229–1244, 2017, doi: 10.1039/c6qm00335d.

[75] L. Jin, X. Zhao, J. Xu, Y. Luo, D. Chen, and G. Chen, "The synergistic effect of a

View Article Online
DOI: 10.1039/D4NA00572D

graphene nanoplate/Fe3O4@BaTiO3 hybrid and MWCNTs on enhancing broadband electromagnetic interference shielding performance," *RSC Adv.*, vol. 8, no. 4, pp. 2065–2071, 2018, doi: 10.1039/c7ra12909b.

[76] P. Sambyal, S. K. Dhawan, P. Gairola, S. S. Chauhan, and S. P. Gairola, "Synergistic effect of polypyrrole/BST/RGO/Fe3O4 composite for enhanced microwave absorption and EMI shielding in X-Band," *Curr. Appl. Phys.*, vol. 18, no. 5, pp. 611–618, 2018, doi: 10.1016/j.cap.2018.03.001.

[77] S. Das, S. Sharma, T. Yokozeki, and S. Dhakate, "Conductive layer-based multifunctional structural composites for electromagnetic interference shielding," *Compos. Struct.*, vol. 261, no. October 2020, p. 113293, 2021, doi: 10.1016/j.compstruct.2020.113293.

[78] X. Jin *et al.*, "Flame-retardant poly(vinyl alcohol)/MXene multilayered films with outstanding electromagnetic interference shielding and thermal conductive performances," *Chem. Eng. J.*, vol. 380, no. August 2019, p. 122475, 2020, doi: 10.1016/j.cej.2019.122475.

[79] Y. Bhattacharjee, I. Arief, and S. Bose, "Recent trends in multi-layered architectures towards screening electromagnetic radiation: Challenges and perspectives," *J. Mater. Chem. C*, vol. 5, no. 30, pp. 7390–7403, 2017, doi: 10.1039/c7tc02172k.

[80] J. H. Lin, Z. I. Lin, Y. J. Pan, C. L. Huang, C. K. Chen, and C. W. Lou, "Polymer composites made of multi-walled carbon nanotubes and graphene nano-sheets: Effects of sandwich structures on their electromagnetic interference shielding effectiveness," *Compos. Part B Eng.*, vol. 89, pp. 424–431, 2016, doi: 10.1016/j.compositesb.2015.11.014.

[81] L. Q. Zhang *et al.*, "Tunable electromagnetic interference shielding effectiveness via multilayer assembly of regenerated cellulose as a supporting substrate and carbon nanotubes/polymer as a functional layer," *J. Mater. Chem. C*, vol. 5, no. 12, pp. 3130–3138, 2017, doi: 10.1039/c6tc05516h.

[82] Y. Hu, P. Tang, L. Li, J. Yang, X. Jian, and Y. Bin, "High absorption shielding material of poly(phthalazinone etherketone)/multiwall carbon nanotube composite films with sandwich configurations," *RSC Adv.*, vol. 9, no. 33, pp. 18758–18766, 2019, doi: 10.1039/c9ra02959a.

[83] S. Pande, B. P. Singh, R. B. Mathur, T. L. Dhami, P. Saini, and S. K. Dhawan,

"Improved electromagnetic interference shielding properties of MWCNT-PMMA composites using layered structures," *Nanoscale Res. Lett.*, vol. 4, no. 4, pp. 327–334, 2009, doi: 10.1007/s11671-008-9246-x.

[84] X. Feng *et al.*, "High Electromagnetic Interference Shielding Effectiveness of Carbon Nanotube–Cellulose Composite Films with Layered Structures," *Macromol. Mater. Eng.*, vol. 303, no. 11, pp. 1–8, 2018, doi: 10.1002/mame.201800377.

[85] Q. Qi *et al.*, "An Effective Design Strategy for the Sandwich Structure of PVDF/GNP-Ni-CNT Composites with Remarkable Electromagnetic Interference Shielding Effectiveness," *ACS Appl. Mater. Interfaces*, vol. 12, no. 32, pp. 36568–36577, 2020, doi: 10.1021/acsami.0c10600.

[86] Y. Xu, Y. Yang, D. X. Yan, H. Duan, G. Zhao, and Y. Liu, "Flexible and conductive polyurethane composites for electromagnetic shielding and printable circuit," *Chem. Eng. J.*, vol. 360, no. July, pp. 1427–1436, 2019, doi: 10.1016/j.cej.2018.10.235.

[87] X. Zhang *et al.*, "Ordered multilayer film of (graphene oxide/polymer and boron nitride/polymer) nanocomposites: An ideal EMI shielding material with excellent electrical insulation and high thermal conductivity," *Compos. Sci. Technol.*, vol. 136, pp. 104–110, 2016, doi: 10.1016/j.compscitech.2016.10.008.

[88] Y. Zhan *et al.*, "An anisotropic layer-by-layer carbon nanotube/boron nitride/rubber composite and its application in electromagnetic shielding," *Nanoscale*, vol. 12, no. 14, pp. 7782–7791, 2020, doi: 10.1039/c9nr10672c.

[89] Y. Bhattacharjee, V. Bhingardive, S. Biswas, and S. Bose, "Construction of a carbon fiber based layer-by-layer (LbL) assembly-a smart approach towards effective EMI shielding," *RSC Adv.*, vol. 6, no. 113, pp. 112614–112619, 2016, doi: 10.1039/C6RA24238C.

[90] S. Biswas, S. S. Panja, and S. Bose, "Unique Multilayered Assembly Consisting of 'flower-Like' Ferrite Nanoclusters Conjugated with MWCNT as Millimeter Wave Absorbers," *J. Phys. Chem. C*, vol. 121, no. 26, pp. 13998–14009, 2017, doi: 10.1021/acs.jpcc.7b02668.

[91] I. Arief, Y. Bhattacharjee, O. Prakash, M. Sahu, S. Suwas, and S. Bose, "Tunable CoNi microstructures in flexible multilayered polymer films can shield electromagnetic radiation," *Compos. Part B Eng.*, vol. 177, no. May, p. 107283, 2019, doi: 10.1016/j.compositesb.2019.107283.

View Article Online
DOI: 10.1039/D4NA00572D

[92] S. Li, Z. Xu, Y. Dong, D. Liu, and G. Sui, "Ni@nylon mesh/PP composites with a novel tree-ring structure for enhancing electromagnetic shielding," *Compos. Part A Appl. Sci. Manuf.*, vol. 131, p. 105798, 2020, doi: 10.1016/j.compositesa.2020.105798.

[93] J. D. Sudha, S. Sivakala, K. Patel, and P. Radhakrishnan Nair, "Development of electromagnetic shielding materials from the conductive blends of polystyrene polyaniline-clay nanocomposite," *Compos. Part A Appl. Sci. Manuf.*, vol. 41, no. 11, pp. 1647–1652, 2010, doi: 10.1016/j.compositesa.2010.07.015.

[94] Y. Xu, Y. Yang, D. X. Yan, H. Duan, G. Zhao, and Y. Liu, "Gradient Structure Design of Flexible Waterborne Polyurethane Conductive Films for Ultraefficient Electromagnetic Shielding with Low Reflection Characteristic," *ACS Appl. Mater. Interfaces*, vol. 10, no. 22, pp. 19143–19152, 2018, doi: 10.1021/acsami.8b05129.

[95] H. Duan *et al.*, "Effect of carbon nanofiller dimension on synergistic EMI shielding network of epoxy/metal conductive foams," *Compos. Part A Appl. Sci. Manuf.*, vol. 118, no. November 2018, pp. 41–48, 2019, doi: 10.1016/j.compositesa.2018.12.016.

[96] W. Ren *et al.*, "Flexible and robust silver coated non-woven fabric reinforced waterborne polyurethane films for ultra-efficient electromagnetic shielding," *Compos. Part B Eng.*, vol. 184, p. 107745, 2020, doi: 10.1016/j.compositesb.2020.107745.

[97] J. Yang *et al.*, "Gradient structure design of lightweight and flexible silicone rubber nanocomposite foam for efficient electromagnetic interference shielding," *Chem. Eng. J.*, vol. 390, p. 124589, 2020, doi: 10.1016/j.cej.2020.124589.

[98] H. Duan *et al.*, "Asymmetric conductive polymer composite foam for absorption dominated ultra-efficient electromagnetic interference shielding with extremely low reflection characteristics," *J. Mater. Chem. A*, vol. 8, no. 18, pp. 9146–9159, 2020, doi: 10.1039/d0ta01393e.

[99] H. J. Im, J. Y. Oh, S. Ryu, and S. H. Hong, "The design and fabrication of a multilayered graded GNP/Ni/PMMA nanocomposite for enhanced EMI shielding behavior," *RSC Adv.*, vol. 9, no. 20, pp. 11289–11295, 2019, doi: 10.1039/C9RA00573K.

[100] A. Sheng *et al.*, "Multilayer WPU conductive composites with controllable electro-magnetic gradient for absorption-dominated electromagnetic interference shielding," *Compos. Part A Appl. Sci. Manuf.*, vol. 129, p. 105692, 2020, doi: 10.1016/j.compositesa.2019.105692.

View Article Online
DOI: 10.1039/D4NA00572D

[101] M. Y. Yablokov, V. G. Shevchenko, L. A. Mukhortov, and A. N. Ozerin, "Electromagnetic interference shielding of carbon nanotube-fluoropolymer elastomer composites with layered structure," *Fullerenes Nanotub. Carbon Nanostructures*, vol. 28, no. 4, pp. 267–271, 2020, doi: 10.1080/1536383X.2019.1697685.

[102] Y. Cai *et al.*, "Electrical conductivity and electromagnetic shielding properties of Ti3SiC2/SiC functionally graded materials prepared by positioning impregnation," *J. Eur. Ceram. Soc.*, vol. 39, no. 13, pp. 3643–3650, 2019, doi: 10.1016/j.jeurceramsoc.2019.05.039.

[103] M. Chen, Y. Zhu, Y. Pan, H. Kou, H. Xu, and J. Guo, "Gradient multilayer structural design of CNTs/SiO2 composites for improving microwave absorbing properties," *Mater. Des.*, vol. 32, no. 5, pp. 3013–3016, 2011, doi: 10.1016/j.matdes.2010.12.043.

[104] X. Ma, Q. Zhang, Z. Luo, X. Lin, and G. Wu, "A novel structure of Ferro-Aluminum based sandwich composite for magnetic and electromagnetic interference shielding," *Mater. Des.*, vol. 89, pp. 71–77, 2016, doi: 10.1016/j.matdes.2015.09.137.

[105] R. Kumar *et al.*, "Heteroatom doping of 2D graphene materials for electromagnetic interference shielding: a review of recent progress," *Crit. Rev. Solid State Mater. Sci.*, vol. 0, no. 0, pp. 1–50, 2021, doi: 10.1080/10408436.2021.1965954.

[106] N. Chen, X. Huang, and L. Qu, "Heteroatom substituted and decorated graphene: Preparation and applications," *Phys. Chem. Chem. Phys.*, vol. 17, no. 48, pp. 32077–32098, 2015, doi: 10.1039/c5cp04391c.

[107] K. Zhang, J. Luo, N. Yu, M. Gu, and X. Sun, "Synthesis and excellent electromagnetic absorption properties of reduced graphene oxide/PANI/BaNd0.2Sm0.2Fe11.6O19 nanocomposites," *J. Alloys Compd.*, vol. 779, pp. 270–279, 2019, doi: 10.1016/j.jallcom.2018.11.284.

[108] Y. Zhang *et al.*, "Fabrication and investigation on the ultra-thin and flexible Ti3C2Tx/co-doped polyaniline electromagnetic interference shielding composite films," *Compos. Sci. Technol.*, vol. 183, no. September, p. 107833, 2019, doi: 10.1016/j.compscitech.2019.107833.

[109] K. Zhang, J. Luo, N. Yu, M. Gu, and X. Sun, "Synthesis and excellent electromagnetic absorption properties of reduced graphene oxide/PANI/BaNd0.2Sm0.2Fe11.6O19 nanocomposites," *J. Alloys Compd.*, vol. 779,

View Article Online
DOI: 10.1039/D4NA00572D

pp. 270–279, 2019, doi: 10.1016/j.jallcom.2018.11.284.

[110] S. Khasim, "Polyaniline-Graphene nanoplatelet composite films with improved conductivity for high performance X-band microwave shielding applications," *Results Phys.*, vol. 12, no. October 2018, pp. 1073–1081, 2019, doi: 10.1016/j.rinp.2018.12.087.

[111] T. Omura, C. H. Chan, M. Wakisaka, and H. Nishida, "Organic Thin Paper of Cellulose Nanofiber/Polyaniline Doped with (±)-10-Camphorsulfonic Acid Nanohybrid and Its Application to Electromagnetic Shielding," *ACS Omega*, vol. 4, no. 5, pp. 9446–9452, 2019, doi: 10.1021/acsomega.9b00708.

[112] S. S. Seyyed Afghahi, R. Peymanfar, S. Javanshir, Y. Atassi, and M. Jafarian, "Synthesis, characterization and microwave characteristics of ternary nanocomposite of MWCNTs/doped Sr-hexaferrite/PANI," *J. Magn. Magn. Mater.*, vol. 423, pp. 152–157, 2017, doi: 10.1016/j.jmmm.2016.09.082.

[113] P. Chamoli, S. K. Singh, M. J. Akhtar, M. K. Das, and K. K. Kar, "Nitrogen doped graphene nanosheet-epoxy nanocomposite for excellent microwave absorption," *Phys. E Low-Dimensional Syst. Nanostructures*, vol. 103, pp. 25–34, 2018, doi: 10.1016/j.physe.2018.05.020.

[114] H. Kadkhodayan, M. S. Seyed Dorraji, M. H. Rasoulifard, A. R. Amani-Ghadim, I. Hajimiri, and A. R. Tarighati Sareshkeh, "Enhanced microwave absorption property of MnFe9n+3O15n+4(0≤n≤1) (M = Ba, Sr)/CaCu3Ti4O12/ phosphorus-doped g-C3N4 nanocomposite: Preparation and optimization," *J. Alloys Compd.*, vol. 735, no. 2018, pp. 2497–2506, 2018, doi: 10.1016/j.jallcom.2017.12.017.

[115] M. Saini, R. Shukla, and A. Kumar, "Cd2+ substituted nickel ferrite doped polyaniline nanocomposites as effective shield against electromagnetic radiation in X-band frequency," *J. Magn. Magn. Mater.*, vol. 491, no. June, p. 165549, 2019, doi: 10.1016/j.jmmm.2019.165549.

[116] Y. F. Liu, L. M. Feng, Y. F. Chen, Y. D. Shi, X. D. Chen, and M. Wang, "Segregated polypropylene/cross-linked poly(ethylene-co-1-octene)/multi-walled carbon nanotube nanocomposites with low percolation threshold and dominated negative temperature coefficient effect: Towards electromagnetic interference shielding and thermisto," *Compos. Sci. Technol.*, vol. 159, pp. 152–161, 2018, doi: 10.1016/j.compscitech.2018.02.041.

[117] A. Nasr Esfahani, A. A. Katbab, A. Taeb, L. Simon, and M. A. Pope, "Correlation between mechanical dissipation and improved X-band electromagnetic shielding capabilities of amine functionalized graphene/thermoplastic polyurethane composites," *Eur. Polym. J.*, vol. 95, no. August, pp. 520–538, 2017, doi: 10.1016/j.eurpolymj.2017.08.038.

[118] J. Abraham *et al.*, "Investigation into dielectric behaviour and electromagnetic interference shielding effectiveness of conducting styrene butadiene rubber composites containing ionic liquid modified MWCNT," *Polymer (Guildf).*, vol. 112, pp. 102–115, 2017, doi: 10.1016/j.polymer.2017.01.078.

[119] J. P. Soares da Silva, B. G. Soares, S. Livi, and G. M. O. Barra, "Phosphonium–based ionic liquid as dispersing agent for MWCNT in melt-mixing polystyrene blends: Rheology, electrical properties and EMI shielding effectiveness," *Mater. Chem. Phys.*, vol. 189, pp. 162–168, 2017, doi: 10.1016/j.matchemphys.2016.12.073.

[120] T. Kaur, S. Kumar, S. B. Narang, and A. K. Srivastava, "Radiation losses in microwave Ku region by conducting pyrrole/barium titanate and barium hexaferrite based nanocomposites," *J. Magn. Magn. Mater.*, vol. 420, pp. 336–342, 2016, doi: 10.1016/j.jmmm.2016.07.058.

[121] S. Araby, A. Qiu, R. Wang, Z. Zhao, C. H. Wang, and J. Ma, "Aerogels based on carbon nanomaterials," *J. Mater. Sci.*, vol. 51, no. 20, pp. 9157–9189, 2016, doi: 10.1007/s10853-016-0141-z.

[122] S. S. Kistler, "Coherent expanded aerogels," *J. Phys. Chem.*, vol. 36, no. 1, pp. 52–64, 1932, doi: 10.1021/j150331a003.

[123] P. Song *et al.*, "Lightweight, Flexible Cellulose-Derived Carbon Aerogel@Reduced Graphene Oxide/PDMS Composites with Outstanding EMI Shielding Performances and Excellent Thermal Conductivities," *Nano-Micro Lett.*, vol. 13, no. 1, 2021, doi: 10.1007/s40820-021-00624-4.

[124] M. T. Noman *et al.*, "Aerogels for biomedical, energy and sensing applications," *Gels*, vol. 7, no. 4, pp. 1–17, 2021, doi: 10.3390/gels7040264.

[125] L. Wang, H. Xu, J. Gao, J. Yao, and Q. Zhang, "Recent progress in metal-organic frameworks-based hydrogels and aerogels and their applications," *Coord. Chem. Rev.*, vol. 398, p. 213016, 2019, doi: 10.1016/j.ccr.2019.213016.

[126] P. Hu *et al.*, "Multifunctional Aramid Nanofiber/Carbon Nanotube Hybrid Aerogel

Films," *ACS Nano*, vol. 14, no. 1, pp. 688–697, 2020, doi: 10.1021/acsnano.9b07459.

[127] F. Xie, K. Gao, L. Zhuo, F. Jia, Q. Ma, and Z. Lu, "Robust Ti3C2Tx/RGO/ANFs hybrid aerogel with outstanding electromagnetic shielding performance and compression resilience," *Compos. Part A Appl. Sci. Manuf.*, vol. 160, no. June, p. 107049, 2022, doi: 10.1016/j.compositesa.2022.107049.

[128] S. Zhao, Y. Yan, A. Gao, S. Zhao, J. Cui, and G. Zhang, "Flexible Polydimethylsilane Nanocomposites Enhanced with a Three-Dimensional Graphene/Carbon Nanotube Bicontinuous Framework for High-Performance Electromagnetic Interference Shielding," *ACS Appl. Mater. Interfaces*, vol. 10, no. 31, pp. 26723–26732, 2018, doi: 10.1021/acsami.8b09275.

[129] L. Q. Zhang *et al.*, *Ultralight Cellulose Porous Composites with Manipulated Porous Structure and Carbon Nanotube Distribution for Promising Electromagnetic Interference Shielding*, vol. 10, no. 46. 2018.

[130] S. Zhao *et al.*, "Highly Electrically Conductive Three-Dimensional Ti3C2Tx MXene/Reduced Graphene Oxide Hybrid Aerogels with Excellent Electromagnetic Interference Shielding Performances," *ACS Nano*, vol. 12, no. 11, pp. 11193–11202, 2018, doi: 10.1021/acsnano.8b05739.

[131] F. Xu *et al.*, "Superflexible Interconnected Graphene Network Nanocomposites for High-Performance Electromagnetic Interference Shielding," *ACS Omega*, vol. 3, no. 3, pp. 3599–3607, 2018, doi: 10.1021/acsomega.8b00432.

[132] Z. Zeng *et al.*, "Ultralight and Flexible Polyurethane/Silver Nanowire Nanocomposites with Unidirectional Pores for Highly Effective Electromagnetic Shielding," *ACS Appl. Mater. Interfaces*, vol. 9, no. 37, pp. 32211–32219, 2017, doi: 10.1021/acsami.7b07643.

[133] X. H. Li *et al.*, "Thermally Annealed Anisotropic Graphene Aerogels and Their Electrically Conductive Epoxy Composites with Excellent Electromagnetic Interference Shielding Efficiencies," *ACS Appl. Mater. Interfaces*, vol. 8, no. 48, pp. 33230–33239, 2016, doi: 10.1021/acsami.6b12295.

[134] X. Wu *et al.*, "Compressible, durable and conductive polydimethylsiloxane-coated MXene foams for high-performance electromagnetic interference shielding," *Chem. Eng. J.*, vol. 381, no. July 2019, p. 122622, 2020, doi: 10.1016/j.cej.2019.122622.

[135] W. Gao *et al.*, "High-efficiency electromagnetic interference shielding realized in

nacre-mimetic graphene/polymer composite with extremely low graphene loading," *Carbon N. Y.*, vol. 157, pp. 570–577, 2020, doi: 10.1016/j.carbon.2019.10.051.

[136] L. Wang *et al.*, "3D Ti3C2Tx MXene/C hybrid foam/epoxy nanocomposites with superior electromagnetic interference shielding performances and robust mechanical properties," *Compos. Part A Appl. Sci. Manuf.*, vol. 123, no. April, pp. 293–300, 2019, doi: 10.1016/j.compositesa.2019.05.030.

[137] Y. Chen, H. Bin Zhang, M. Wang, X. Qian, A. Dasari, and Z. Z. Yu, "Phenolic resin-enhanced three-dimensional graphene aerogels and their epoxy nanocomposites with high mechanical and electromagnetic interference shielding performances," *Compos. Sci. Technol.*, vol. 152, pp. 254–262, 2017, doi: 10.1016/j.compscitech.2017.09.022.

[138] J. F. Wang, S. Q. Shi, J. P. Yang, and W. Zhang, "Multiscale analysis on free vibration of functionally graded graphene reinforced PMMA composite plates," *Appl. Math. Model.*, vol. 98, pp. 38–58, 2021, doi: 10.1016/j.apm.2021.04.023.

[139] Y. Yang, M. C. Gupta, K. L. Dudley, and R. W. Lawrence, "Novel carbon nanotube - Polystyrene foam composites for electromagnetic interference shielding," *Nano Lett.*, vol. 5, no. 11, pp. 2131–2134, 2005, doi: 10.1021/nl051375r.

[140] X. Ma, B. Shen, L. Zhang, Y. Liu, W. Zhai, and W. Zheng, "Porous superhydrophobic polymer/carbon composites for lightweight and self-cleaning EMI shielding application," *Compos. Sci. Technol.*, vol. 158, pp. 86–93, 2018, doi: 10.1016/j.compscitech.2018.02.006.

[141] L. Ma, M. Hamidinejad, L. Wei, B. Zhao, and C. B. Park, "Absorption-dominant EMI shielding polymer composite foams: Microstructure and geometry optimization," *Mater. Today Phys.*, vol. 30, no. November 2022, 2023, doi: 10.1016/j.mtphys.2022.100940.

[142] H. Zhang, G. Zhang, Q. Gao, M. Zong, M. Wang, and J. Qin, "Electrically electromagnetic interference shielding microcellular composite foams with 3D hierarchical graphene-carbon nanotube hybrids," *Compos. Part A Appl. Sci. Manuf.*, vol. 130, p. 105773, 2020, doi: 10.1016/j.compositesa.2020.105773.

[143] H. Zhang *et al.*, "Multifunctional microcellular PVDF/Ni-chains composite foams with enhanced electromagnetic interference shielding and superior thermal insulation performance," *Chem. Eng. J.*, vol. 379, no. April 2019, p. 122304, 2020, doi:

View Article Online
DOI: 10.1039/D4NA00572D

10.1016/j.cej.2019.122304.

[144] J. Yang *et al.*, "Light-weight and flexible silicone rubber/MWCNTs/Fe3O4 nanocomposite foams for efficient electromagnetic interference shielding and microwave absorption," *Compos. Sci. Technol.*, vol. 181, no. January, p. 107670, 2019, doi: 10.1016/j.compscitech.2019.05.027.

[145] L. Liu, H. Wang, M. Shan, Y. Jiang, X. Zhang, and Z. Xu, "Lightweight sandwich fiber-welded foam-like nonwoven fabrics/graphene composites for electromagnetic shielding," *Mater. Chem. Phys.*, vol. 232, no. April, pp. 246–253, 2019, doi: 10.1016/j.matchemphys.2019.04.085.

[146] X. Fan *et al.*, "Study on foamability and electromagnetic interference shielding effectiveness of supercritical CO 2 foaming epoxy/rubber/MWCNTs composite," *Compos. Part A Appl. Sci. Manuf.*, vol. 121, no. March, pp. 64–73, 2019, doi: 10.1016/j.compositesa.2019.03.008.

[147] H. Zhang *et al.*, "Synergistic effect of carbon nanotube and graphene nanoplates on the mechanical, electrical and electromagnetic interference shielding properties of polymer composites and polymer composite foams," *Chem. Eng. J.*, vol. 353, no. May, pp. 381–393, 2018, doi: 10.1016/j.cej.2018.07.144.

[148] H. Yuan, Y. Xiong, Q. Shen, G. Luo, D. Zhou, and L. Liu, "Synthesis and electromagnetic absorbing performances of CNTs/PMMA laminated nanocomposite foams in X-band," *Compos. Part A Appl. Sci. Manuf.*, vol. 107, no. January, pp. 334–341, 2018, doi: 10.1016/j.compositesa.2018.01.024.

[149] S. E. Zakiyan, H. Azizi, and I. Ghasemi, "Effect of cell morphology on electrical properties and electromagnetic interference shielding of graphene-poly(methyl methacrylate) microcellular foams," *Compos. Sci. Technol.*, vol. 157, pp. 217–227, 2018, doi: 10.1016/j.compscitech.2018.02.002.

[150] J. Li *et al.*, "Electrical conductivity and electromagnetic interference shielding of epoxy nanocomposite foams containing functionalized multi-wall carbon nanotubes," *Appl. Surf. Sci.*, vol. 428, pp. 7–16, 2018, doi: 10.1016/j.apsusc.2017.08.234.

[151] H. Zhang *et al.*, "Lightweight, multifunctional microcellular PMMA/Fe3O4@MWCNTs nanocomposite foams with efficient electromagnetic interference shielding," *Compos. Part A Appl. Sci. Manuf.*, vol. 100, pp. 128–138,

2017, doi: 10.1016/j.compositesa.2017.05.009.

[152] M. Soltani Alkuh, M. H. N. Famili, M. Mokhtari Motameni Shirvan, and M. H. Moeini, "The relationship between electromagnetic absorption properties and cell structure of poly(methyl methacrylate)/multi-walled carbon nanotube composite foams," *Mater. Des.*, vol. 100, pp. 73–83, 2016, doi: 10.1016/j.matdes.2016.03.075.

[153] J. Li *et al.*, "Morphologies and electromagnetic interference shielding performances of microcellular epoxy/multi-wall carbon nanotube nanocomposite foams," *Compos. Sci. Technol.*, vol. 129, pp. 70–78, 2016, doi: 10.1016/j.compscitech.2016.04.003.

[154] G. Gedler, M. Antunes, J. I. Velasco, and R. Ozisik, "Enhanced electromagnetic interference shielding effectiveness of polycarbonate/graphene nanocomposites foamed via 1-step supercritical carbon dioxide process," *Mater. Des.*, vol. 90, pp. 906–914, 2016, doi: 10.1016/j.matdes.2015.11.021.

[155] B. Zhao *et al.*, "Achieving wideband microwave absorption properties in PVDF nanocomposite foams with an ultra-low MWCNT content by introducing a microcellular structure," *J. Mater. Chem. C*, vol. 8, no. 1, pp. 58–70, 2019, doi: 10.1039/c9tc04575a.

[156] B. Zhao *et al.*, "Incorporating a microcellular structure into PVDF/graphene-nanoplatelet composites to tune their electrical conductivity and electromagnetic interference shielding properties," *J. Mater. Chem. C*, vol. 6, no. 38, pp. 10292–10300, 2018, doi: 10.1039/C8TC03714K.

[157] F. Huang *et al.*, "Oxidized multiwall carbon nanotube/silicone foam composites with effective electromagnetic interference shielding and high gamma radiation stability," *RSC Adv.*, vol. 8, no. 43, pp. 24236–24242, 2018, doi: 10.1039/c8ra03314e.

[158] C. Zhang *et al.*, "Facile fabrication of ultra-light and highly resilient PU/RGO foams for microwave absorption," *RSC Adv.*, vol. 7, no. 66, pp. 41321–41329, 2017, doi: 10.1039/c7ra07794g.

[159] C. Liang *et al.*, "Constructing interconnected spherical hollow conductive networks in silver platelets/reduced graphene oxide foam/epoxy nanocomposites for superior electromagnetic interference shielding effectiveness," *Nanoscale*, vol. 11, no. 46, pp. 22590–22598, 2019, doi: 10.1039/c9nr06022g.

[160] X. Sun, X. Liu, X. Shen, Y. Wu, Z. Wang, and J. K. Kim, "Graphene foam/carbon

DOI: 10.1039/D4NA00572D

nanotube/poly(dimethyl siloxane) composites for exceptional microwave shielding," *Compos. Part A Appl. Sci. Manuf.*, vol. 85, pp. 199–206, 2016, doi: 10.1016/j.compositesa.2016.03.009.

[161] J. Liu, J. Cheng, R. Che, J. Xu, M. Liu, and Z. Liu, "Double-shelled yolk-shell microspheres with Fe3O4 cores and SnO2 double shells as high-performance microwave absorbers," *J. Phys. Chem. C*, vol. 117, no. 1, pp. 489–495, 2013, doi: 10.1021/jp310898z.

[162] I. Arief, S. Biswas, and S. Bose, "Wool-Ball-Type Core-Dual-Shell FeCo@SiO2@MWCNTs Microcubes for Screening Electromagnetic Interference," *ACS Appl. Nano Mater.*, vol. 1, no. 5, pp. 2261–2271, 2018, doi: 10.1021/acsanm.8b00333.

[163] L. yan Li, S. lin Li, Y. Shao, R. Dou, B. Yin, and M. bo Yang, "PVDF/PS/HDPE/MWCNTs/Fe3O4 nanocomposites: Effective and lightweight electromagnetic interference shielding material through the synergetic effect of MWCNTs and Fe3O4 nanoparticles," *Curr. Appl. Phys.*, vol. 18, no. 4, pp. 388–396, 2018, doi: 10.1016/j.cap.2018.01.014.

[164] K. Manna and S. K. Srivastava, "Fe3O4@Carbon@Polyaniline Trilaminar Core-Shell Composites as Superior Microwave Absorber in Shielding of Electromagnetic Pollution," *ACS Sustain. Chem. Eng.*, vol. 5, no. 11, pp. 10710–10721, 2017, doi: 10.1021/acssuschemeng.7b02682.

[165] S. Li, Y. Huang, N. Zhang, M. Zong, and P. Liu, "Synthesis of polypyrrole decorated FeCo@SiO2 as a high-performance electromagnetic absorption material," *J. Alloys Compd.*, vol. 774, pp. 532–539, 2019, doi: 10.1016/j.jallcom.2018.09.349.

[166] Y. Bhattacharjee, D. Chatterjee, and S. Bose, "Core-Multishell Heterostructure with Excellent Heat Dissipation for Electromagnetic Interference Shielding," *ACS Appl. Mater. Interfaces*, vol. 10, no. 36, pp. 30762–30773, 2018, doi: 10.1021/acsami.8b10819.

[167] L. Wang *et al.*, "Electromagnetic interference shielding MWCNT-Fe3O4@Ag/epoxy nanocomposites with satisfactory thermal conductivity and high thermal stability," *Carbon N. Y.*, vol. 141, pp. 506–514, 2019, doi: 10.1016/j.carbon.2018.10.003.

[168] Y. Yuan *et al.*, "Lightweight, flexible and strong core-shell non-woven fabrics covered by reduced graphene oxide for high-performance electromagnetic

View Article Online
DOI: 10.1039/D4NA00572D

interference shielding," *Carbon N. Y.*, vol. 130, pp. 59–68, 2018, doi: 10.1016/j.carbon.2017.12.122.

[169] Y. Wang, W. Zhang, C. Luo, X. Wu, G. Yan, and W. Chen, "Fabrication and high-performance microwave absorption of Ni@SnO2 @PPy Core-Shell composite," *Synth. Met.*, vol. 220, pp. 347–355, 2016, doi: 10.1016/j.synthmet.2016.07.005.

[170] H. K. Choudhary, R. Kumar, S. P. Pawar, U. Sundararaj, and B. Sahoo, "Enhancing absorption dominated microwave shielding in co@c-pvdf nanocomposites through improved magnetization and graphitization of the co@c-nanoparticles," *Phys. Chem. Chem. Phys.*, vol. 21, no. 28, pp. 15595–15608, 2019, doi: 10.1039/c9cp03305j.

[171] X. P. Zhang, L. C. Jia, G. Zhang, D. X. Yan, and Z. M. Li, "A highly efficient and heat-resistant electromagnetic interference shielding carbon nanotube/poly(phenylene sulfide) composite via sinter molding," *J. Mater. Chem. C*, vol. 6, no. 40, pp. 10760–10766, 2018, doi: 10.1039/C8TC03493A.

[172] R. Sun *et al.*, "Highly Conductive Transition Metal Carbide/Carbonitride(MXene)@polystyrene Nanocomposites Fabricated by Electrostatic Assembly for Highly Efficient Electromagnetic Interference Shielding," *Adv. Funct. Mater.*, vol. 27, no. 45, pp. 1–11, 2017, doi: 10.1002/adfm.201702807.

[173] K. Zhang *et al.*, "A facile approach to constructing efficiently segregated conductive networks in poly(lactic acid)/silver nanocomposites via silver plating on microfibers for electromagnetic interference shielding," *Compos. Sci. Technol.*, vol. 156, pp. 136–143, 2018, doi: 10.1016/j.compscitech.2017.12.037.

[174] J. Ju *et al.*, "Lightweight multifunctional polypropylene/carbon nanotubes/carbon black nanocomposite foams with segregated structure, ultralow percolation threshold and enhanced electromagnetic interference shielding performance," *Compos. Sci. Technol.*, vol. 193, 2020, doi: 10.1016/j.compscitech.2020.108116.

[175] J. Chen, X. Liao, W. Xiao, J. Yang, Q. Jiang, and G. Li, "Facile and Green Method to Structure Ultralow-Threshold and Lightweight Polystyrene/MWCNT Composites with Segregated Conductive Networks for Efficient Electromagnetic Interference Shielding," *ACS Sustain. Chem. Eng.*, vol. 7, no. 11, pp. 9904–9915, 2019, doi: 10.1021/acssuschemeng.9b00678.

View Article Online
DOI: 10.1039/D4NA00572D

[176] Y. J. Tan *et al.*, "Comparative study on solid and hollow glass microspheres for enhanced electromagnetic interference shielding in polydimethylsiloxane/multi-walled carbon nanotube composites," *Compos. Part B Eng.*, vol. 177, no. August, p. 107378, 2019, doi: 10.1016/j.compositesb.2019.107378.

[177] F. Sharif, M. Arjmand, A. A. Moud, U. Sundararaj, and E. P. L. Roberts, "Segregated Hybrid Poly(methyl methacrylate)/Graphene/Magnetite Nanocomposites for Electromagnetic Interference Shielding," *ACS Appl. Mater. Interfaces*, vol. 9, no. 16, pp. 14171–14179, 2017, doi: 10.1021/acsami.6b13986.

[178] Y. Zhan *et al.*, "Enhancing the EMI shielding of natural rubber-based supercritical CO 2 foams by exploiting their porous morphology and CNT segregated networks," *Nanoscale*, vol. 11, no. 3, pp. 1011–1020, 2019, doi: 10.1039/c8nr07351a.

[179] W. C. Yu *et al.*, *Constructing highly oriented segregated structure towards high-strength carbon nanotube/ultrahigh-molecular-weight polyethylene composites for electromagnetic interference shielding*, vol. 110. Elsevier Ltd, 2018.

[180] K. Zhang *et al.*, "A facile approach to constructing efficiently segregated conductive networks in poly(lactic acid)/silver nanocomposites via silver plating on microfibers for electromagnetic interference shielding," *Compos. Sci. Technol.*, vol. 156, pp. 136–143, 2018, doi: 10.1016/j.compscitech.2017.12.037.

[181] H. Wang *et al.*, "3D network porous polymeric composites with outstanding electromagnetic interference shielding," *Compos. Sci. Technol.*, vol. 125, pp. 22–29, 2016, doi: 10.1016/j.compscitech.2016.01.007.

[182] K. Zhang *et al.*, "Ultralow percolation threshold and enhanced electromagnetic interference shielding in poly(l-lactide)/multi-walled carbon nanotube nanocomposites with electrically conductive segregated networks," *J. Mater. Chem. C*, vol. 5, no. 36, pp. 9359–9369, 2017, doi: 10.1039/c7tc02948a.

[183] P. Song *et al.*, "Honeycomb structural rGO-MXene/epoxy nanocomposites for superior electromagnetic interference shielding performance," *Sustain. Mater. Technol.*, vol. 24, p. e00153, 2020, doi: 10.1016/j.susmat.2020.e00153.

[184] V. T. Nguyen, B. K. Min, Y. Yi, S. J. Kim, and C. G. Choi, "MXene(Ti3C2TX)/graphene/PDMS composites for multifunctional broadband electromagnetic interference shielding skins," *Chem. Eng. J.*, vol. 393, p. 124608, 2020, doi: 10.1016/j.cej.2020.124608.

[185] P. Song *et al.*, "Obviously improved electromagnetic interference shielding performances for epoxy composites via constructing honeycomb structural reduced graphene oxide," *Compos. Sci. Technol.*, vol. 181, no. June, p. 107698, 2019, doi: 10.1016/j.compscitech.2019.107698.

[186] H. Fang, H. Guo, Y. Hu, Y. Ren, P. C. Hsu, and S. L. Bai, "In-situ grown hollow Fe3O4 onto graphene foam nanocomposites with high EMI shielding effectiveness and thermal conductivity," *Compos. Sci. Technol.*, vol. 188, p. 107975, 2020, doi: 10.1016/j.compscitech.2019.107975.

[187] C. Liang *et al.*, "Highly oriented three-dimensional structures of Fe3O4 decorated CNTs/reduced graphene oxide foam/epoxy nanocomposites against electromagnetic pollution," *Compos. Sci. Technol.*, vol. 181, no. June, p. 107683, 2019, doi: 10.1016/j.compscitech.2019.107683.

[188] Y. Huangfu *et al.*, "Fabrication and investigation on the PANI/MWCNT/thermally annealed graphene aerogel/epoxy electromagnetic interference shielding nanocomposites," *Compos. Part A Appl. Sci. Manuf.*, vol. 121, no. March, pp. 265–272, 2019, doi: 10.1016/j.compositesa.2019.03.041.

[189] Y. Huangfu *et al.*, "Fabrication and investigation on the Fe3O4/thermally annealed graphene aerogel/epoxy electromagnetic interference shielding nanocomposites," *Compos. Sci. Technol.*, vol. 169, no. November 2018, pp. 70–75, 2019, doi: 10.1016/j.compscitech.2018.11.012.

[190] J. Ouyang, Q. Xu, C. W. Chu, Y. Yang, G. Li, and J. Shinar, "On the mechanism of conductivity enhancement in poly(3,4- ethylenedioxythiophene):poly(styrene sulfonate) film through solvent treatment," *Polymer (Guildf).*, vol. 45, no. 25, pp. 8443–8450, 2004, doi: 10.1016/j.polymer.2004.10.001.

[191] C. Lan, M. Guo, C. Li, Y. Qiu, Y. Ma, and J. Sun, "Axial Alignment of Carbon Nanotubes on Fibers to Enable Highly Conductive Fabrics for Electromagnetic Interference Shielding," *ACS Appl. Mater. Interfaces*, vol. 12, no. 6, pp. 7477–7485, 2020, doi: 10.1021/acsami.9b21698.

[192] J. P L, H. Nallabothula, A. V. Menon, and S. Bose, "Nanoinfiltration for Enhancing Microwave Attenuation in Polystyrene-Nanoparticle Composites," *ACS Appl. Nano Mater.*, vol. 3, no. 2, pp. 1872–1880, 2020, doi: 10.1021/acsanm.9b02521.

[193] R. Salehiyan, M. Nofar, S. S. Ray, and V. Ojijo, "Kinetically Controlled Localization of

Carbon Nanotubes in Polylactide/Poly(vinylidene fluoride) Blend Nanocomposites and Their Influence on Electromagnetic Interference Shielding, Electrical Conductivity, and Rheological Properties," *J. Phys. Chem. C*, vol. 123, no. 31, pp. 19195–19207, 2019, doi: 10.1021/acs.jpcc.9b04494.

[194] S. M. N. Sultana, S. P. Pawar, and U. Sundararaj, "Effect of Processing Techniques on EMI SE of Immiscible PS/PMMA Blends Containing MWCNT: Enhanced Intertube and Interphase Scattering," *Ind. Eng. Chem. Res.*, vol. 58, no. 26, pp. 11576–11584, 2019, doi: 10.1021/acs.iecr.8b05957.

[195] H. Nallabothula, Y. Bhattacharjee, L. Samantara, and S. Bose, "Processing-Mediated Different States of Dispersion of Multiwalled Carbon Nanotubes in PDMS Nanocomposites Influence EMI Shielding Performance," *ACS Omega*, vol. 4, no. 1, pp. 1781–1790, 2019, doi: 10.1021/acsomega.8b02920.

[196] S. P. Pawar, P. Rzeczkowski, P. Pötschke, B. Krause, and S. Bose, "Does the Processing Method Resulting in Different States of an Interconnected Network of Multiwalled Carbon Nanotubes in Polymeric Blend Nanocomposites Affect EMI Shielding Properties?," *ACS Omega*, vol. 3, no. 5, pp. 5771–5782, 2018, doi: 10.1021/acsomega.8b00575.

[197] R. Rohini and S. Bose, "Extraordinary Improvement in Mechanical Properties and Absorption-Driven Microwave Shielding through Epoxy-Grafted Graphene 'interconnects,'" *ACS Omega*, vol. 3, no. 3, pp. 3200–3210, 2018, doi: 10.1021/acsomega.7b01997.

[198] W. Xu, Y. F. Pan, W. Wei, and G. S. Wang, "Nanocomposites of Oriented Nickel Chains with Tunable Magnetic Properties for High-Performance Broadband Microwave Absorption," *ACS Appl. Nano Mater.*, vol. 1, no. 3, pp. 1116–1123, 2018, doi: 10.1021/acsanm.7b00293.

[199] J. Hua *et al.*, "Graphene/MWNT/Poly(p-phenylenebenzobisoxazole) Multiphase Nanocomposite via Solution Prepolymerization with Superior Microwave Absorption Properties and Thermal Stability," *J. Phys. Chem. C*, vol. 121, no. 2, pp. 1072–1081, 2017, doi: 10.1021/acs.jpcc.6b11925.

[200] S. Biswas, G. P. Kar, and S. Bose, "Tailor-Made Distribution of Nanoparticles in Blend Structure toward Outstanding Electromagnetic Interference Shielding," *ACS Appl. Mater. Interfaces*, vol. 7, no. 45, pp. 25448–25463, 2015, doi:

View Article Online
DOI: 10.1039/D4NA00572D

10.1021/acsami.5b08333.

[201] J. Pre-proofs, "Flexible polyethylene terephthalate / polyaniline composite," 2020.

[202] Y. M. Li, C. Deng, Z. Y. Zhao, L. X. Han, P. Lu, and Y. Z. Wang, "Carbon fiber-based polymer composite via ceramization toward excellent electromagnetic interference shielding performance and high temperature resistance," *Compos. Part A Appl. Sci. Manuf.*, vol. 131, 2020, doi: 10.1016/j.compositesa.2020.105769.

[203] S. H. Lee *et al.*, "Low percolation 3D Cu and Ag shell network composites for EMI shielding and thermal conduction," *Compos. Sci. Technol.*, vol. 182, no. June, 2019, doi: 10.1016/j.compscitech.2019.107778.

[204] A. Gebrekrstos, S. Biswas, A. V. Menon, G. Madras, P. Pötschke, and S. Bose, "Multi-layered stack consisting of PVDF nanocomposites with flow-induced oriented MWCNT structure can supress electromagnetic radiation," *Compos. Part B Eng.*, vol. 166, no. February, pp. 749–757, 2019, doi: 10.1016/j.compositesb.2019.03.008.

[205] R. Ravindren, S. Mondal, K. Nath, and N. C. Das, "Investigation of electrical conductivity and electromagnetic interference shielding effectiveness of preferentially distributed conductive filler in highly flexible polymer blends nanocomposites," *Compos. Part A Appl. Sci. Manuf.*, vol. 118, pp. 75–89, 2019, doi: 10.1016/j.compositesa.2018.12.012.

[206] N. K. Hota, N. Karna, K. A. Dubey, D. K. Tripathy, and B. P. Sahoo, "Effect of temperature and electron beam irradiation on the dielectric properties and electromagnetic interference shielding effectiveness of ethylene acrylic elastomer/millable polyurethane/SWCNT nanocomposites," *Eur. Polym. J.*, vol. 112, pp. 754–765, 2019, doi: 10.1016/j.eurpolymj.2018.10.048.

[207] D. P. Schmitz *et al.*, "Electromagnetic interference shielding effectiveness of ABS carbon-based composites manufactured via fused deposition modelling," *Mater. Today Commun.*, vol. 15, no. February, pp. 70–80, 2018, doi: 10.1016/j.mtcomm.2018.02.034.

[208] K. Chizari, M. Arjmand, Z. Liu, U. Sundararaj, and D. Therriault, "Three-dimensional printing of highly conductive polymer nanocomposites for EMI shielding applications," *Mater. Today Commun.*, vol. 11, pp. 112–118, 2017, doi: 10.1016/j.mtcomm.2017.02.006.

View Article Online
DOI: 10.1039/D4NA00572D

[209] K. Zhang *et al.*, "Morphological regulation improved electrical conductivity and electromagnetic interference shielding in poly(l-lactide)/poly(ε-caprolactone)/carbon nanotube nanocomposites via constructing stereocomplex crystallites," *J. Mater. Chem. C*, vol. 5, no. 11, pp. 2807–2817, 2017, doi: 10.1039/c7tc00389g.

[210] A. D. La Rosa *et al.*, "Recovery of electronic wastes as fillers for electromagnetic shielding in building components: An LCA study," *J. Clean. Prod.*, vol. 280, p. 124593, 2021, doi: 10.1016/j.jclepro.2020.124593.

[211] M. Rahaman, I. A. Al Ghufais, G. Periyasami, and A. Aldalbahi, "Recycling and Reusing Polyethylene Waste as Antistatic and Electromagnetic Interference Shielding Materials," *Int. J. Polym. Sci.*, vol. 2020, 2020, doi: 10.1155/2020/6421470.

[212] A. V. Menon, G. Madras, and S. Bose, " Mussel-Inspired Self-Healing Polyurethane with 'Flower-like' Magnetic MoS 2 as Efficient Microwave Absorbers ," *ACS Appl. Polym. Mater.*, vol. 1, no. 9, pp. 2417–2429, 2019, doi: 10.1021/acsapm.9b00538.

[213] A. V. Menon, G. Madras, and S. Bose, "Ultrafast Self-Healable Interfaces in Polyurethane Nanocomposites Designed Using Diels-Alder 'click' as an Efficient Microwave Absorber," *ACS Omega*, vol. 3, no. 1, pp. 1137–1146, 2018, doi: 10.1021/acsomega.7b01845.

[214] A. V. Menon, B. Choudhury, G. Madras, and S. Bose, "'Trigger-free' self-healable electromagnetic shielding material assisted by co-doped graphene nanostructures," *Chem. Eng. J.*, vol. 382, p. 122816, 2020, doi: 10.1016/j.cej.2019.122816.

[215] P. Yan *et al.*, "Recyclable, self-healing, absorption-dominated and highly effective electromagnetic shielding elastomers based on bridged micro capacitance structure," *Carbon N. Y.*, vol. 166, pp. 56–63, 2020, doi: 10.1016/j.carbon.2020.04.091.

[216] X. Dai *et al.*, "Recoverable and self-healing electromagnetic wave absorbing nanocomposites," *Compos. Sci. Technol.*, vol. 174, no. February, pp. 27–32, 2019, doi: 10.1016/j.compscitech.2019.02.018.

[217] S. Li, J. Li, N. Ma, D. Liu, and G. Sui, "Super-Compression-Resistant Multiwalled Carbon Nanotube/Nickel-Coated Carbonized Loofah Fiber/Polyether Ether Ketone Composite with Excellent Electromagnetic Shielding Performance," *ACS Sustain.*

View Article Online
DOI: 10.1039/D4NA00572D

Chem. Eng., vol. 7, no. 16, pp. 13970–13980, 2019, doi: 10.1021/acssuschemeng.9b02447.

[218] H. Fang *et al.*, “Simultaneous improvement of mechanical properties and electromagnetic interference shielding performance in eco-friendly polylactide composites via reactive blending and MWCNTs induced morphological optimization,” *Compos. Part B Eng.*, vol. 178, no. September, p. 107452, 2019, doi: 10.1016/j.compositesb.2019.107452.

[219] S. Kashi, R. K. Gupta, T. Baum, N. Kao, and S. N. Bhattacharya, “Dielectric properties and electromagnetic interference shielding effectiveness of graphene-based biodegradable nanocomposites,” *Mater. Des.*, vol. 109, pp. 68–78, 2016, doi: 10.1016/j.matdes.2016.07.062.

[220] G. Wang, G. Zhao, S. Wang, L. Zhang, and C. B. Park, “Injection-molded microcellular PLA/graphite nanocomposites with dramatically enhanced mechanical and electrical properties for ultra-efficient EMI shielding applications,” *J. Mater. Chem. C*, vol. 6, no. 25, pp. 6847–6859, 2018, doi: 10.1039/c8tc01326h.

[221] G. Wang *et al.*, “Ultralow-Threshold and Lightweight Biodegradable Porous PLA/MWCNT with Segregated Conductive Networks for High-Performance Thermal Insulation and Electromagnetic Interference Shielding Applications,” *ACS Appl. Mater. Interfaces*, vol. 10, no. 1, pp. 1195–1203, 2018, doi: 10.1021/acsami.7b14111.

[222] S. Kashi, R. K. Gupta, T. Baum, N. Kao, and S. N. Bhattacharya, “Morphology, electromagnetic properties and electromagnetic interference shielding performance of poly lactide/graphene nanoplatelet nanocomposites,” *Mater. Des.*, vol. 95, pp. 119–126, 2016, doi: 10.1016/j.matdes.2016.01.086.

[223] T. Kuang, L. Chang, F. Chen, Y. Sheng, D. Fu, and X. Peng, “Facile preparation of lightweight high-strength biodegradable polymer/multi-walled carbon nanotubes nanocomposite foams for electromagnetic interference shielding,” *Carbon N. Y.*, vol. 105, pp. 305–313, 2016, doi: 10.1016/j.carbon.2016.04.052.

[224] D. A. Gopakumar *et al.*, “Cellulose Nanofiber-Based Polyaniline Flexible Papers as Sustainable Microwave Absorbers in the X-Band,” *ACS Appl. Mater. Interfaces*, vol. 10, no. 23, pp. 20032–20043, 2018, doi: 10.1021/acsami.8b04549.

[225] Z. Wang *et al.*, “Paper-based metasurface: Turning waste-paper into a solution for

View Article Online
DOI: 10.1039/D4NA00572D

electromagnetic pollution," *J. Clean. Prod.*, vol. 234, pp. 588–596, 2019, doi: 10.1016/j.jclepro.2019.06.239.

[226] L. Vazhayal, P. Wilson, and K. Prabhakaran, "Waste to wealth: Lightweight, mechanically strong and conductive carbon aerogels from waste tissue paper for electromagnetic shielding and CO2 adsorption," *Chem. Eng. J.*, vol. 381, no. August 2019, p. 122628, 2020, doi: 10.1016/j.cej.2019.122628.

[227] P. J. Bora, M. Porwal, K. J. Vinoy, Kishore, P. C. Ramamurthy, and G. Madras, "Industrial waste fly ash cenosphere composites based broad band microwave absorber," *Compos. Part B Eng.*, vol. 134, pp. 151–163, 2018, doi: 10.1016/j.compositesb.2017.09.062.

[228] P. J. Bora, N. Mallik, P. C. Ramamurthy, Kishore, and G. Madras, "Poly(vinyl butyral) -polyaniline-magnetically functionalized fly ash cenosphere composite film for electromagnetic interference shielding," *Compos. Part B Eng.*, vol. 106, pp. 224–233, 2016, doi: 10.1016/j.compositesb.2016.09.035.

[229] P. Lv *et al.*, "Metal-based bacterial cellulose of sandwich nanomaterials for anti-oxidation electromagnetic interference shielding," *Mater. Des.*, vol. 112, pp. 374–382, 2016, doi: 10.1016/j.matdes.2016.09.100.

[230] G. George *et al.*, "Green and facile approach to prepare polypropylene/: In situ reduced graphene oxide nanocomposites with excellent electromagnetic interference shielding properties," *RSC Adv.*, vol. 8, no. 53, pp. 30412–30428, 2018, doi: 10.1039/c8ra05007d.

View Article Online
DOI: 10.1039/D4NA00572D

A Review on recent progress in polymer composites for effective electromagnetic interference shielding properties- Structures, Process, Sustainability approaches

Rajesh Kumar Bheema[1], Krithika Bhaskaran[1], Akshat Verma[1], Gopu J[1], Murthy Chavali[2] and Krishna Chaitanya Etika[1]*

[1] Department of Chemical Engineering, BITS Pilani, Pilani, Rajasthan 333 031, India
[2] Office of the Dean Research, MIT World Peace University, Survey No, 124, Paud Rd, Kothrud, Pune, Maharashtra 411038, India

* Corresponding author emails: etika.krishna@pilani.bits-pilani.ac.in

Data Availability Statement

No primary research results, software or code have been included and no new data were generated or analysed as part of this review